Contents:

Materials. All solvents were dried using standard procedures; all other reagents were reagent grade quality obtained from commercial suppliers and used without further purification. Melting points are uncorrected. NMR spectra were recorded at 600, 400, and 300 MHz for ^{1}H and 100 MHz for ^{13}C. Chemical shifts are expressed in ppm (δ) using the residual solvent signal as an internal reference (7.16 ppm for C_6H_6; 7.26 ppm for $CHCl_3$ and 3.31 for CD_2HOD). Mass spectra were recorded in the ESI mode. Compounds CX,[1] 1a,b,[2] 2b,[3] 3a,b[4] and 4a,b[5] were synthesised according to published procedures.

Methods.

UV/Vis Spectroscopy. All spectroscopic measurements were performed on air-equilibrated CH_2Cl_2 (Uvasol) solutions at room temperature. UV/Vis spectra were recorded with a Cary 300 (Agilent) spectrophotometer.

Electrochemical measurements. Cyclic voltammetric (CV) and differential pulse voltammetric (DPV) experiments were carried out in argon-purged CH_2Cl_2 (Sigma-Aldrich) with an Autolab 30 multipurpose instrument interfaced to a PC. The working electrode was a glassy carbon electrode (Amel, 0.07 cm^2), carefully polished with an alumina-water slurry on a felt surface immediately before use. The counter electrode was a Pt wire, separated from the solution by a frit, and an Ag wire was employed as a quasi-reference electrode, and ferrocene was present as an internal standard. The concentration of the examined compounds was ranging from 0.05 to 0.3 mM. Tetrabutylammonium hexafluorophosphate ($TBAPF_6$) was added in a 100-fold proportion with respect to the sample concentration, as supporting electrolyte. Cyclic voltammograms were obtained at scan rates varying from 50 to 1000 mV s^{-1}. Differential pulse voltammetries were performed with a scan rate of 20 mV s^{-1} (pulse height 75 mV). The IR compensation was used, and every effort was made throughout the experiments in order to minimise the resistance of the solution. The electrochemical reversibility of the voltammetric wave of ferrocene was taken as an indicator of the absence of uncompensated resistance effects.

Synthetic Procedures

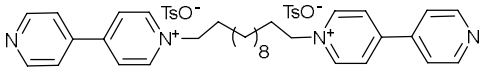

DC-4 5b

Bis(pyridylpyridinium) ditosylate 5b (DC-4): in a 100 mL round bottomed flask, a solution of ditosylate 2b (0.50 g, 0.98 mmol) and 4,4'-bipyridyl (0.38 g, 2.45 mmol) in dry CH_3CN (40 mL) was refluxed under stirring for 24 h. After this period, the solution was cooled to room temperature and then evaporated to dryness under reduced pressure. The resulting solid residue was then recrystallised from CH_3OH to afford 0.46 g of 5b as a white sticky solid compound (57 %). ^{1}H NMR (CD_3OD, 400 MHz) δ (ppm) = 9.11 (d, 4H, ^{3}J = 6.3 Hz), 8.84 (d, 4H, ^{3}J = 4.6 Hz), 8.51 (d, 4H, ^{3}J = 4.0 Hz), 7.99 (d, 4H, ^{3}J = 6.2 Hz), 7.71 (d, 4H, ^{3}J = 6.7 Hz), 7.23 (d, 4H ^{3}J = 7.1), 4.68 (t, 4H, ^{3}J = 7.5 Hz), 2.37 (s, 6H), 2.13-2.00 (m, 4H), 1.5-1.3 (m, 16H); ^{13}C NMR (CD_3OD, 100 MHz): δ (ppm) = 153.5, 150.4, 145.1, 142.2, 140.3, 128.5, 126.9,125.7, 125.5, 121.7, 61.3, 31.1, 29.2, 29.1, 28.8, 25.9, 19.9. MS (ESI): m/z: 240.1 $[M-2TsO]^{2+}$.

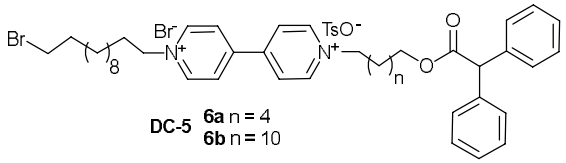

DC-5 **6a** n = 4
6b n = 10

General procedure for the synthesis of the viologen axles 6a,b (DC-5): in a sealed 100 mL glass autoclave, a solution of the appropriate salt 4a,b (0.3 mmol) and 1,12-dibromododecane (0.46 g, 1.4 mmol) in dry CH_3CN (40 mL) were refluxed under vigorous stirring for 7 days. Afterwards, the solution was cooled to room temperature to allow the precipitation of the desired product upon standing.

6a: 0.15 g (52 %) were isolated after the precipitation as a pale-yellow solid compound. M.p. >250 °C (dec.); ^{1}H NMR (CD_3OD, 600 MHz) δ (ppm) = 9.27 (d, 2H, ^3J = 6.5 Hz), 9.24 (d, 2H, ^3J = 6.7 Hz), 8.63-8.69 (m, 4H), 7.68 (d, 1H, ^3J = 8.1 Hz), 7.20-7.33 (m, 11H), 5.07 (s, 1H), 4.74 (t, 2H, ^3J = 7.6 Hz), 4.69 (t, 2H, ^3J = 7.5 Hz), 4.16 (t, 2H, ^3J = 6.5 Hz), 3.43 (t, 2H, ^3J = 6.7 Hz), 2.36 (s, 1.5H), 2.13-2.06 (m, 2H), 2.05-1.99 (m, 2H), 1.80-1.86 (m, 2H), 1.69-1.63 (m, 2H), 1.5-1.3 (m, 20H); ^{13}C NMR (100 MHz): δ (ppm) = 174.3, 151.3, 147.0, 143.7, 141.8, 140.3,129.9, 129.3, 128.7, 128.3 (two res.), 126.9, 65.8, 63.3, 63.1, 58.2, 34.5, 33.9, 32.6, 32.3, 30.6, 30.5 (two res.), 30.1, 29.8, 29.2, 29.1, 27.3, 26.5, 26.2, 21.3; MS (ESI): m/z: 350.3 $[M\text{-}2X]^{2+}$.

6b: 0.13 g (47 %) were isolated after the precipitation as a pale-yellow solid compound. M.p. >250 °C (dec.); ^{1}H NMR (CD_3OD, 600 MHz) δ (ppm) = 9.27 (d, 4H, ^3J = 6.2 Hz), 8.67 (d, 4H, ^3J = 5.6 Hz), 7.67 (d, 1H, ^3J = 8.2 Hz), 7.20-7.33 (m, 11H), 5.07 (s, 1H), 4.74 (t, 4H, ^3J = 7.6 Hz), 4.14 (t, 2H, ^3J = 6.5 Hz), 3.43 (t, 2H, ^3J = 6.7 Hz), 2.36 (s, 1H), 2.13-2.06 (m, 4H), 1.79-1.89 (m, 2H), 1.63-1.57 (m, 2H), 1.5-1.2 (m, 32H); ^{13}C NMR (100 MHz): δ (ppm) = 171.4, 150.0, 145.8, 139.0, 128.5, 128.4, 128.2, 127.0, 126.9, 125.6, 64.9, 62.0, 57.0, 33.1, 32.6, 31.2, 29.2 (four res.), 29.1 (two res.), 28.8, 28.5, 27.8, 25.9, 25.0, 20.0. MS (ESI): m/z: 392.2 $[M\text{-}2X]^{2+}$.

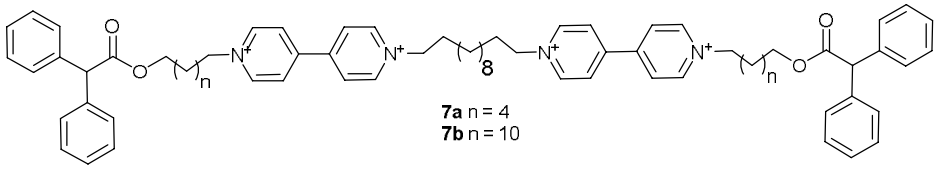

7a n = 4
7b n = 10

General procedure for the synthesis of the dumbbell 7a,b: in a sealed 100 mL glass autoclave, a solution of the appropriate pyridylpyridinium salt 4a,b (0.33 mmol) and ditosylate 2b (0.056 g, 0.11 mmol) in dry CH_3CN (40 mL) was refluxed under vigorous stirring for 7 days. The solution was then cooled to room temperature to allow the precipitation of the desired product.

7a: 0.14 g (74 %) were isolated after precipitation as a white solid compound. M.p.= 225.4-225.9 °C; ^{1}H NMR (CD_3OD, 400 MHz): δ (ppm) = 9.24 (d, 4H, ^3J = 6.9 Hz), 9.21 (d, 4H, ^3J = 7.2 Hz), 8.64 (d, 8H, ^3J = 6.0 Hz), 7.69 (d, 8H, ^3J = 8.2 Hz), 7.36-7.20 (m, 28H), 5.09 (s, 2H), 4.72 (t, 4H, ^3J = 7.6 Hz), 4.67 (t, 4H, ^3J = 7.5 Hz), 4.17 (t, 4H, ^3J = 6.5 Hz), 2.37 (s, 12H), 2.12-2.05 (m, 4H), 1.70–1.59 (m, 4H), 1.5-1.3 (m, 26H); ^{13}C NMR (100 MHz): δ (ppm) = 172.8, 149.8, 145.6, 142.2, 140.3, 138.9, 128.5, 128.3, 128.2 (two res.), 126.9 (two res.), 125.5, 64.4, 61.9, 61.7, 56.8, 31.2, 30.9, 29.2, 29.1, 28.8, 27.9, 25.9, 25.1, 24.8, 19.9. MS (ESI): m/z: 267.7$[M\text{-}4TsO]^{4+}$.

7b: 0.15 g (71 %) were isolated after precipitation as a white solid compound. M.p.= 237.7-238.3 °C; ^{1}H NMR (CD_3OD, 400 MHz): δ (ppm) = 9.22 (d, 8H, ^{3}J = 6.6 Hz), 8.63 (d, 8H, ^{3}J = 6.5 Hz), 7.69 (d, 8H, ^{3}J = 8.2 Hz), 7.37-7.18 (m, 28H), 5.09 (s, 2H), 4.71 (t, 8H, ^{3}J = 7.6 Hz), 4.15 (t, 4H, ^{3}J = 6.4 Hz), 2.36 (s, 12H), 2.11–1.99 (m, 8H), 1.60 (t, 4H, ^{3}J = 6.5 Hz), 1.5-1.2 (m, 48H); ^{13}C NMR (100 MHz): δ (ppm) = 172.9, 149.7, 145.6, 142.3, 140.3, 138.9, 128.5, 128.3, 128.2 (two res.), 126.9 (two res.), 125.5, 64.8, 61.9, 56.9, 31.2, 31.1, 29.2 (four res.), 29.1 (two res.), 28.8, 28.2, 25.8, 25.5, 20.0; MS (ESI): m/z: 309.7$[M\text{-}4TsO]^{4+}$.

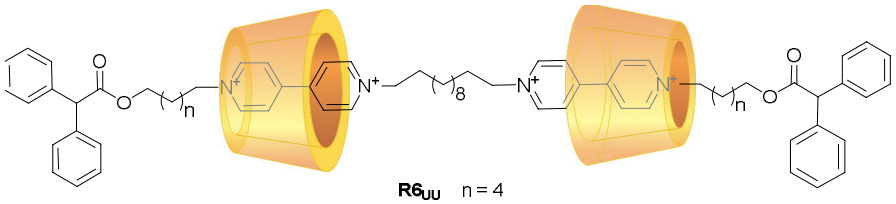

$R6_{UU}$ n = 4
$R12_{UU}$ n = 10

General procedure for the synthesis of the [3]rotaxanes orientational isomers UU: in a sealed glass tube, the appropriate dumbbell component DC-2 (4a,b) (0.14 mmol) was suspended in 2 mL of dry toluene, then wheel CX (0.22 g, 0.15 mmol) and the ditosylate 2b (31 mg, 0.06 mmol) were added. The mixture was stirred at room temperature until the complete dissolution of the reagents was observed. After stirring at 65 °C for 7 days, the solvent was evaporated under reduced pressure. The crude residue was then purified by column chromatography (Hex:EtOAc:MeOH = 60:35:5). The purified product was then dissolved in 2 mL of dichloromethane, and a solution of AgOTs in ethanol (20 mL) was added. The mixture was stirred for 2 hours, and then the solvent was evaporated to dryness under reduced pressure. The solid residue was taken up in dichloromethane and filtered to remove the silver salts.

$R6_{UU}$ was obtained as a red sticky solid in 62% yield. ^{1}H NMR ($CDCl_3$, 400 MHz): δ (ppm) = 8.9, 8.8, 8.63 and 8.59 (4 br. s, 12H); 7.81 (d, 8H, J = 8.1 Hz); 7.70 (br. s, 4H); 7.58 (br. s., 6H); 7.5-7.3 and 7.43 (m and br. d, 58H, J ~ 7 Hz); 7.20 (d, 8H, J = 8.1 Hz); 7.08 (br. t, 12H, J ~ 6 Hz); 6.92 (br. s, 10H); 6.80 and 6.75 (br. t, br. s, 8H, J ~ 7 Hz); 6.67 and 6.63 (br. d and br. s, 6H, J ~ 4 Hz); 6.24 (br. d, 3H, J ~ 4 Hz); 5.08 and 5.05 (2 br. s, 2H); 4.49 (d, 12H, J = 14.9 Hz); 4.36 (br. t, 4H, J ~ 6.5 Hz); 4.03, 3.96, 3.9, 3.82 and 3.75 (br. s, s, br. s, br. s, 60 H); 3.62 (q, 12H, J = 6.9 Hz); 3.46 (d, 12H, J = 14.9 Hz); 3.22 (br. t, 4H); 2.82 (br. s., 1H); 2.38 (s, 12H); 2.03, 1.96, 1.83 and 1.64 (4 br. s., 16H); 1.44 and 1.41 (br. s, s, 58H); 1.34 -1.13 (m, 30H); 1.0, 0.86, 0.76 and 0.66 (4 br. s, 16H); ^{13}C NMR (100 MHz): δ (ppm) = 172.5, 153.2, 152.5, 148.1, 147.6, 145.7, 143.9, 142.7, 142.3, 140.4, 139.9, 138.7, 136.7, 133.8, 131.9, 128.9, 128.8, 128.7, 128.5, 127.4, 126.1, 125.3, 124.2, 121.3, 117.7, 116.6, 72.5, 71.6, 70.0, 66.6, 65.1, 61.2, 60.9, 60.6, 57.2, 34.5, 31.7, 31.3, 29.5, 29.3, 29.1, 28.9, 28.4, 27.8, 26.2, 21.4, 15.4. For complete proton assignment see Fig. S1-S7; HR-MS (ESI, Orbitrap LQ) calculated for $C_{266}H_{316}N_{16}O_{34}S_2$ m/z (z = 2): 2171.14602 (24 %), 2171.64769 (70 %), 2172.14937 (100 %), 2172.65105 (95 %), 2173.15273 (68 %), 2173.65440 (39 %), 2174.15608 (18 %), 2174.65776 (7 %); Found: 271.14727 (21 %), 2171.64984 (64 %), 2172.14021 (97 %), 2172.65105 (100 %), 2173.15302 (80 %), 2173.65450 (55 %), 2174.15436 (31 %), 2174.65442 (15 %).

$R12_{UU}$ was obtained as a red sticky solid in 43% yield. ^{1}H NMR ($CDCl_3$, 400 MHz): δ (ppm) = 8.96, 8.83, 8.63 and 8.60 (4 br. s, 14H); 7.83 and 7.70 (d, br. s., 14H, *J* = 7.8 Hz); 7.6 – 7.2 (m, 60H); 7.21 (d, 8H, *J* = 7.7 Hz); 7.09 (br. t, 15H, *J* ~ 7 Hz); 6.93 (br. s, 10H); 6.9 – 6.7 (m, 11H), 6.6 (br. s, 5H); 60.5 (br. s, 3H); 5.05 (s, 2H); 4.50 (d, 11H, *J* = 14.8 Hz); 4.25 and 4.20 (br. s, t, 9H, *J* = 7.1 Hz); 4.06, 4.00, and 3.87 (3 br. s, 58 H); 3.66 (q, 16H, *J* = 7.1 Hz); 3.47 (d, 13H, *J* = 14.8 Hz); 3.18 (br. t, 4H); 2.86 (br. s., 1H); 2.39 (s, 12H); 2.09 (br. s, 4H); 1.77, 1.68, 1.57, 1.49, 1.41, 1.35, 1.3 - 1.2 and 1.19 (4 br. s, s, br. s, m, br. s, 169H); 0.93, 0.82, 0.72 and 0.65 (4 br. s, 18H); ^{13}C NMR (100 MHz): δ (ppm) = 172.6, 153.1, 152.8, 148.1, 144.0, 142. 7, 142.3, 140.4, 139.9, 138.8, 136.7, 133.9, 131.9, 128.9, 128.8, 128.6 (2 res.), 127.3, 126.1, 125.3, 124.1, 121.4, 117.7, 116.6, 72.5, 71.4, 70.1, 66.7, 65.2, 61.3, 60.6, 57.2, 34.5, 31.7, 31.3, 30.6, 30.2, 29.9, 29.8 (2 res.), 29.7, 29.3, 29.1, 28.9, 28.6, 28.3, 26.2, 25.9, 21.4, 15.4. For complete proton assignment see Fig. S21; HR-MS (ESI, Orbitrap LQ) calculated for $C_{271}H_{333}N_{16}O_{31}S$: m/z (z = 3): 1446.4892 (20 %), 1446.8236 (61 %), 1447.1580 (95 %), 1447.4924 (100 %), 1447.8267 (80 %), 1448.1610 (53 %), 1448.4952 (29 %), 1448.8295 (14 %); Found: 1446.4878 (17 %), 1446.8230 (63 %), 1447.1573 (97 %), 1447.4916 (100 %), 1447.8258 (81 %), 1448.1599 (54 %), 1448.4940 (30 %), 1448.8286 (13 %).

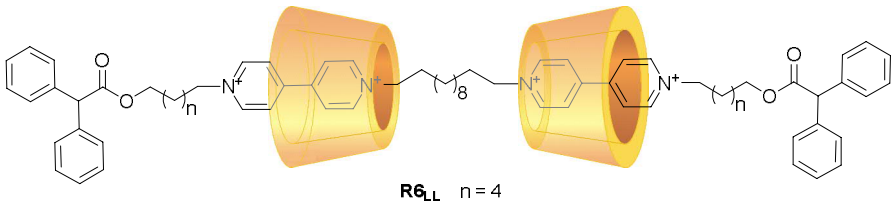

$R6_{LL}$ n = 4
$R12_{LL}$ n = 10

General procedure for the synthesis of the [3]Rotaxanes orientational isomers LL: in a sealed glass tube, dumbbell component DC-4 (5b) (35 mg, 0.043 mmol) was suspended in 2 mL of dry toluene, then wheel CX (170 mg, 0.12 mmol) and the appropriate dumbbell component DC-1 (3a,b) (0.11 mmol) were added. The mixture was stirred at room temperature until the complete dissolution of the reagents. After stirring at 65 °C for 7 days, the solvent was evaporated under reduced pressure. The crude mixture was then purified through column chromatography (Hex:EtOAc:MeOH = 60:35:5). The purified product was then dissolved in 2 mL of dichloromethane, and a solution of AgOTs in ethanol (20 mL) was added. The mixture was stirred for 2 hours, and then the solvent was evaporated to dryness under reduced pressure. The solid residue was taken up in dichloromethane and filtered to remove the silver salts.

$R6_{LL}$ was obtained as a red sticky solid in 50% yield. ^{1}H NMR ($CDCl_3$, 400 MHz): δ (ppm) = 8.63 and 8.60 (2 br. s, 12H); 7.81 (br. d, 8H, *J* ~ 6 Hz); 7.74 (br. s, 4H); 7.62 (br. s., 2H); 7.6-7.3 (m, 48H); 7.26 (m, 8H); 7.20 (d, 8H, *J* = 8 Hz); 7.07 and 7.02 (br. s and br. t, 14H); 6.92 (br. s, 8H); 6.82 and 6.74 (br. d, br. t, 10H); 6.61 and 6.55 (2 br. s, 3H); 6.07, 6.03 and 5.96 (3 br. s, 3H); 5.08, 5.04 and 5.01 (3 br. s, 2H); 4.50 (d, 12H, *J* = 14.9 Hz); 4.3-3.8, 4.08, 4.03 and 3.89 (m, 3 br. s, 64H); 3.69 (q, 12H, *J* = 6.9 Hz); 3.48 (d, 12H, *J* = 14.9 Hz); 3.15 (br. s, 4H); 2.95 (br. s, 1H); 2.39 (s, 12H); 2.14 (br. s, 4H), 1.84, 1.73, 1.64, 1.52, 1.41, 1.31 (4 br. s, s, t, 124H, *J* = 7.2 Hz); 0.99, 0.90, 0.75, 0.65 and 0.58 (5 br. s, 14H); ^{13}C NMR (100 MHz): δ (ppm) = 172.6, 153.1, 152.4, 148.2, 148.1, 144.0, 142.7, 142.0, 140.2, 140.1, 138.7,

136.6, 133.8, 131.9, 129.0, 128.8 (2 res.), 128.7, 128.6, 127.3, 126.1, 125.2, 124.1, 121.4, 117.6, 116.6, 72.5, 70.1, 66.7, 66.6 (2 res.), 65.0, 61.2, 60.2, 57.2, 34.5, 31.8 (2 res.), 31.4, 30.9, 29.7, 29.1, 28.5, 28.4, 28.2, 25.7, 24.9, 21.4, 15.5. For complete proton assignment see Fig. S8-S14; HR-MS (ESI, Orbitrap LQ) calculated for $C_{259}H_{309}N_{16}O_{31}S$: m/z (z = 3): 1390.42663 (26 %), 1390.76108 (72 %), 1391.09554 (100 %), 1391.42999 (92 %), 1391.76444 (64 %), 1392.09889 (36 %), 1392.43334 (16 %), 1392.76779 (7 %), 1393.10224 (2 %); Found: 1390.42712 (23 %), 1390.76050 (66 %), 1391.09497 (100 %), 1391.42957 (89 %), 1391.76392 (76 %), 1392.09778 (39 %), 1392.43201 (23 %), 1392.76831(13 %), 1393.09827 (4 %).

$R12_{LL}$ was obtained as a red sticky solid in 38 % yield. ^{1}H NMR ($CDCl_3$, 400 MHz): δ (ppm) = 8.61 (br. s, 12H); 7.82 and 7.73 (d, br. s, 12H, J = 7.4 Hz); 7.71, 7.56, 7.47, 7.43, 7.41, 7.39, 7.36, 7.34 and 7.3 – 7.2 (6 br. s., 2 s, m, 61H); 7.21 (d, 11H, J = 8 Hz); 7.07 (br. t, 17H, J = 7.15 Hz); 6.94 (br. s, 11H); 6.79 (br. t, 12H, J = 6.7 Hz); 6.61 (br. s, 5H); 6.06 (br. s, 3H); 5.06 (s, 2H); 4.52 (d, 11H, J = 14.5 Hz); 4.27 (br. s, 2H); 4.19 (t, 5H, J = 6.7 Hz); 4.08, 4.03 and 3.89 (br. s, s, br. s, 58H); 3.69 (q, 16H, J = 6.9 Hz); 3.48 (d, 14H, J = 14.9 Hz); 3.15 (br. s, 4H); 2.95 (br. s, 1H); 2.39 (s, 12H); 2.14 (br. s, 3H), 1.85, 1.7 – 1.6, 1.52, 1.4 – 1.2 and 1.15 (br. s, m, br. s, s, m, br. s, 172H); 1.0 – 0.8, 0.78 and 0.61 (m, 2 br. s, 20H); ^{13}C NMR (100 MHz): δ (ppm) = 172.6, 153.1, 152.4, 148.2, 148.1, 147.9, 144.0, 142.7, 142.3, 140.3, 140.0, 138.8, 136.7, 136.1, 134.3, 133.8, 133.1, 131.9, 129.0, 128.8, 128.6 (2 res.), 127.2, 126.1, 125.3, 124.1, 121.4, 117.7, 116.7, 72.5, 70.1, 66.6, 65.4, 61.2, 61.0, 60.6, 57.2, 34.5, 31.8, 31.3, 31.1, 30.9, 30.7, 29.8, 29.7, 29.6, 29.5, 29.4, 29.3, 29.1, 28.7, 28.6, 28.5, 26.1, 25.9, 21.4, 15.4. For complete proton assignment see Fig. S23; HR-MS (ESI, Orbitrap LQ) calculated for $C_{264}H_{326}N_{16}O_{28}$: m/z (z = 4): 1042.11389 (23 %), 1042.36471 (67 %), 1042.6155 (99 %), 1042.86632 (100 %), 1043.11712 (76 %), 1043.36790 (47 %), 1043.61869 (24 %), 1043.86947 (11 %); Found: 1042.11169(22 %), 1042.36292 (69 %), 1042.61365 (100 %), 1042.86543 (94 %), 1043.11462 (77 %), 1043.36560(47 %), 1043.61584 (24 %), 1043.86633(11 %).

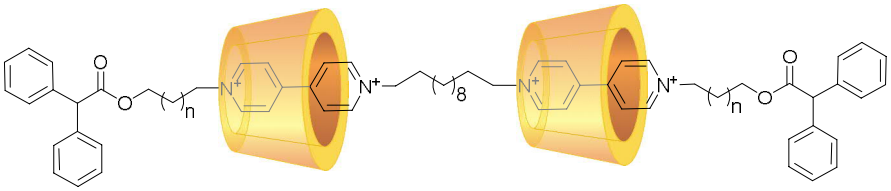

$R6_{UL}$ n = 4
$R12_{UL}$ n = 10

General procedure for the synthesis of the [3]Rotaxanes orientational isomers UL: in a sealed glass tube, the appropriate dumbbell component DC-5 (6a,b) (0.055 mmol) was suspended in 2 mL of dry toluene, wheel CX (0.26 g, 0.176 mmol) was added, and the mixture was stirred at 80 °C for 4 hours. The solution was then cooled to room temperature appropriate dumbbell component DC-2 (4a,b) (0.077 mmol) was added. After stirring at room temperature for 30 min, the mixture was reacted at 80 °C for 7 days. The solvent was evaporated under reduced pressure, and the crude mixture was purified through column chromatography (Hex:EtOAc:MeOH = 60:35: 5). The purified product was then dissolved in 2 mL of dichloromethane, and a solution of AgOTs in ethanol (20 mL) was

added. The mixture was stirred for 2 hours, and then the solvent was evaporated to dryness under reduced pressure. The solid residue was taken up in dichloromethane and filtered to remove the silver salts.

$R6_{UL}$ was obtained as a red sticky solid in 42 % yield. ^{1}H NMR ($CDCl_3$, 400 MHz): δ (ppm) = 8.66 and 8.61 (2 br. s, 12H); 7.83 (br. d, 8H, $J \sim 7$ Hz); 7.64 -7.25 (m, 56H); 7.21 (d, 12H, $J = 7.6$ Hz); 7.08 and 7.02 (2t , 14H, $J = 7.5$ Hz); 6.90 (br. s, 10H); 6.7- 6.5 and 6.39 (m, br. s, 4H); 6.03 and 5.90 (2 br. s, 2H); 5.1, 5.08 and 5.04 (3s, 2H); 4.51 and 4.48 (2d, 12H, $J = 14.4$ Hz); 4.36 (t, 2H, $J = 6.3$ Hz); 4.2 (br. s., 3H), 4.06, 4.02 and 3.97 (2 br. s, s, 35H); 3.89 and 3.83 (2 br. s, 21H); 3.68 and 3.63 (2q, 15H, $J = 6.9$ Hz); 3.46 (d, 12H, $J = 14.5$ Hz); 3.23 (br. s, 2H); 3.11 (br. s, 2H); 2.40 (s, 12H); 2.15 and 2.07 (2 br. s, 4H); 1.95 (br. t, 2H); 1.80 and 1.71 (2 br. s, 15H); 1.6 -1.1 (m, 106H); 0.98, 0.86, 0.72, and 0.57 (4 br. s, 16H); ^{13}C NMR (100 MHz): δ (ppm) = 172.6, 153.08, 152.4, 148.1, 148.0, 144.0, 142.7, 142.2, 140.5, 140.3, 140.0, 138.8, 138.6, 136.6, 135.8, 134.3, 133.3, 133.2, 131.9, 128.9 (2 res.), 128.8 (2 res.), 128.7 (2 res.), 128.6, 128.5, 127.5, 127.3, 126.1, 125.6, 125.3, 124.1, 124.0, 121.4, 121.2, 117.8, 117.7, 116.7, 72.6 (2 res.), 70.1, 70.0, 66.7, 66.6, 65.1, 61.4, 61.3, 60.9, 60.4, 60.2, 57.2, 57.1, 34.5, 31.7 (2 res.), 31.4, 30.8, 30.4, 30.2, 30.1, 29.9, 29.7, 29.6, 29.2, 29.0 (2 res.), 28.4, 27.8, 26.2, 26.1, 25.7, 24.8, 21.4, 15.5, 15.4. For complete proton assignment see Fig. S15-S20; HR-MS (ESI, Orbitrap LQ) calculated for $C_{266}H_{316}N_{16}O_{34}S_2$: m/z (z = 2): 2171.14602 (24 %), 2171.64769 (70 %), 2172.14937 (100 %), 2172.65105 (95 %), 2173.15273 (68 %), 2173.65440 (39 %), 2174.15608 (18 %), 2174.65776 (7 %); Found: 2171.14418 (21 %), 2171.64652 (63 %), 2172.14827 (94 %), 2172.64991 (100 %), 2173.15087 (82 %), 2173.65132 (55 %), 2174.15145 (30 %), 2174.65206 (14 %).

$R12_{UL}$ was obtained as a red sticky solid in 40 % yield. ^{1}H NMR ($CDCl_3$, 400 MHz): δ (ppm) = 9.04, 8.82, 8.68 and 8.56 (2 br. s, 2 s, 12H); 7.82 and 7.6 (br. d, br. s, 12H, $J \sim 7$ Hz); 7.6 – 7.2 (m, 82H); 7.21 (d, 17H, $J = 7.6$ Hz); 7.2 – 7.0 (m , 21H); 6.9 – 6.7 (m, 26H); 6.61 and 6.49 (2 br. s, 3H); 6.00 (br. s, 2H); 5.06 (s, 2H); 4.6 – 4.5 (m, 14H); 4.25 and 4.36 (br. s, t, 10H, $J = 6.7$ Hz); 4.06, 4.02 and 4.00 (br. s, 2 s, 45H); 3.88 (br. s, 35H); 3.7 – 3.6 (m, 24H); 3.47 (bd, 16H, $J = 14$ Hz); 3.17 and 2.95 (2 br. s, 6H); 2.39 (s, 12H); 2.20 (br. s, 4H); 1.79, 1.68, 1.52, 1.49, and 1.44 (5 br. s, 130H); 1.4 – 1.2 (m, 95H); 1.14, 1.00, 0.9 – 0.8, 0.74, 0.63 and 0.54 (2 br. s, m, 3 br. s, 39H); ^{13}C NMR (100 MHz): δ (ppm) =153.1, 152.4, 148.0, 142.7, 138.8, 138.7, 134.0, 132.0, 128.9, 128.8 (2 res.), 128.6 (3 res.), 127.3, 127.2, 126.1, 121.4, 121.2, 117.7, 117.6, 116.5, 72.6, 70.1, 66.7, 65.4, 65.3, 61.4 (2 res.), 57.2 (2 res.), 34.5, 31.4, 30.0, 29.9 (2 res.), 29.7 (2 res), 29.6 (2 res.), 29.3, 29.0, 28.6 (2 res.), 25.9 (2 res.), 21.4, 15.5, 15.4. For complete proton assignment see Fig. S22; HR-MS (ESI, Orbitrap LQ) calculated for $C_{278}H_{340}N_{16}O_{34}S_2$: m/z (z = 2): 2255.23992 (22 %), 2255.74160 (67 %), 2256.24327 (100 %), 2256.74495 (99 %), 2257.246632 (74 %), 2257.74830 (44 %), 2258.24998 (22 %), 2258.75166 (9 %); Found: 2255.23668 (18 %), 2255.74953 (58 %), 2256.24190 (93 %), 2256.74351 (100 %), 2257.246381 (83 %), 2257.74418 (59 %), 2258.24485 (34 %), 2258.74509 (17 %).

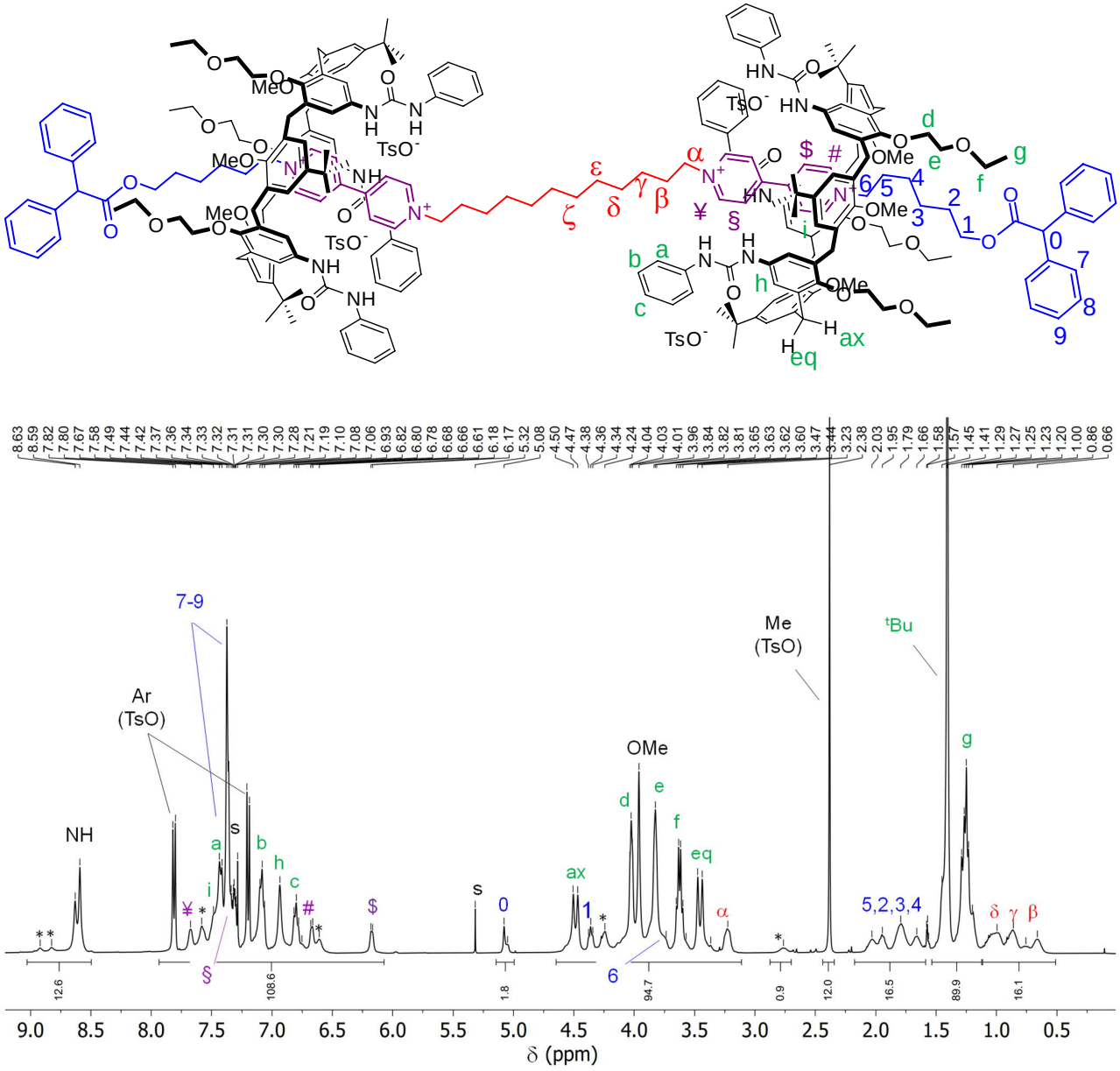

Figure S1. ^{1}H NMR spectrum (400 MHz, $CDCl_3$) of [3]rotaxane $R6_{UU}$. The signals deriving from the *paCo* rotamer are indicated with an asterisk (see Fig. S7).

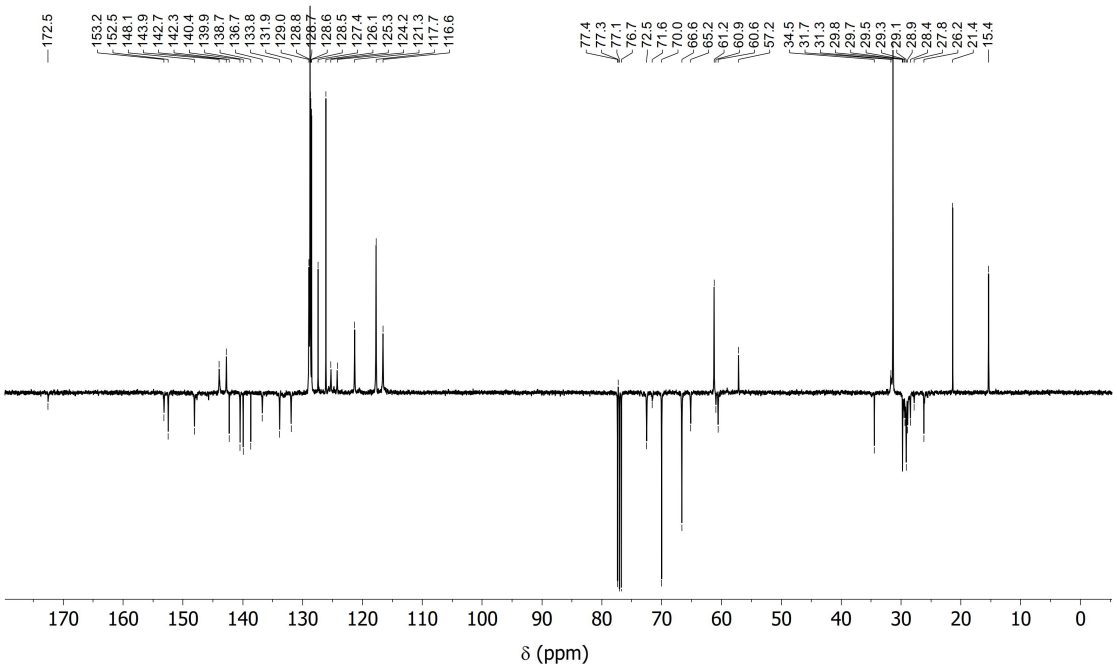

Figure S2. ^{13}C DEPT-Q NMR spectrum (100 MHz, $CDCl_3$) of [3]rotaxane $R6_{UU}$. Positive signals indicate tertiary and primary carbons while the negative the quaternary and secondary ones (solvent signals are negative).

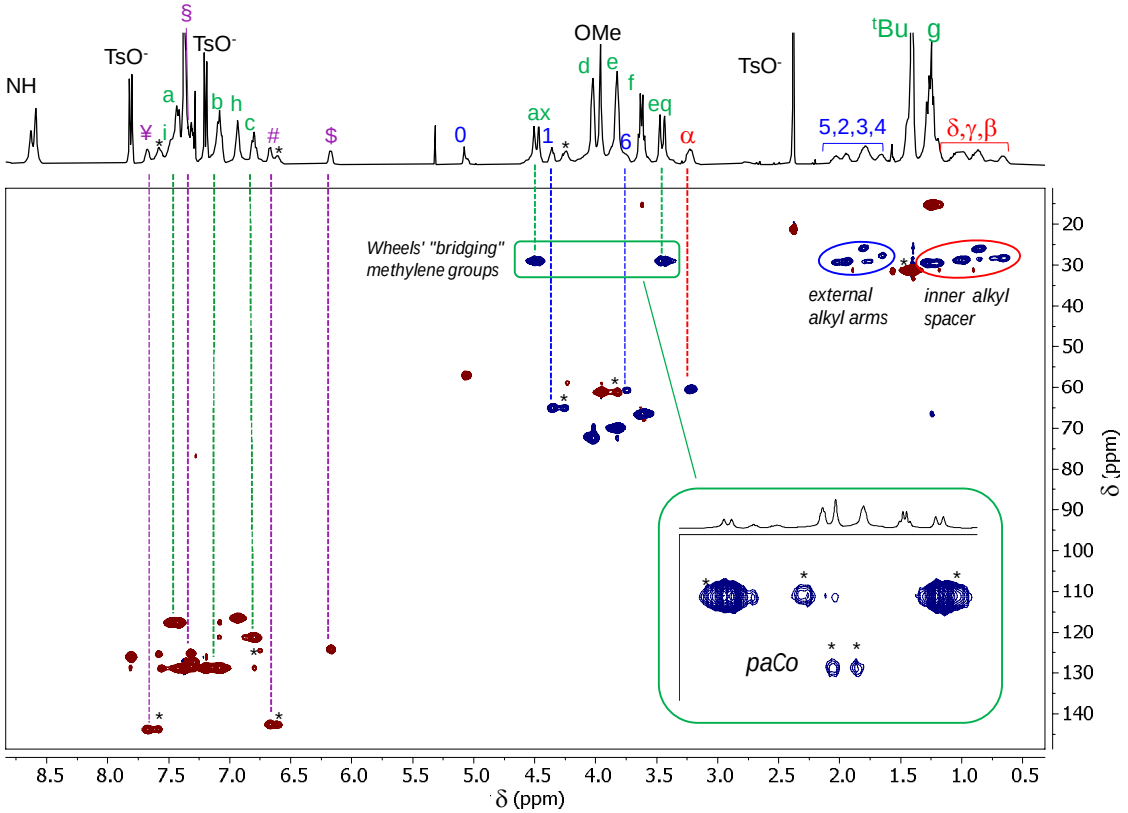

Figure S3. 2D edited HSQC spectrum of [3]rotaxane $R6_{UU}$. The cross-peaks with blue contours indicate CH couplings of tertiary and primary carbons, while those with reddish contours the CH couplings of secondary carbons. The cross-peaks relative to the macrocycles methylene bridging units have been highlighted with a green box, while those relative to the external and internal alkyl chains with blue and red ellipses, respectively. The inset shows the enhanced correlations of the bridging methylene groups of the *paCo* rotamer (all the projection peaks and correlations arising from this rotamer have been indicated with an asterisk).

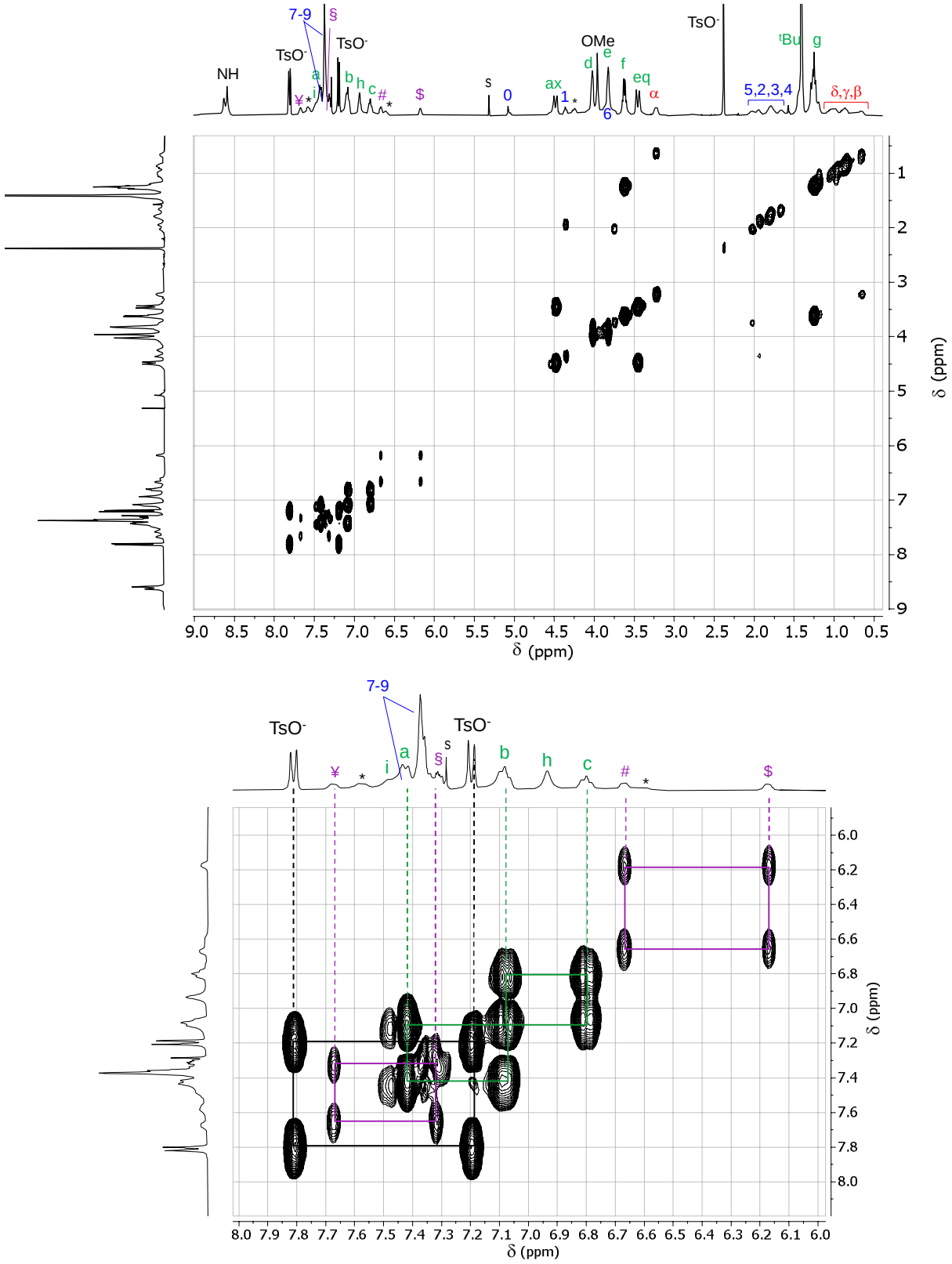

Figure S4. (Top) Magnitude mode 2D DQF-COSY spectrum of $R6_{UU}$ ($CDCl_3$, 400 MHz); (down) Low-fields expansion.

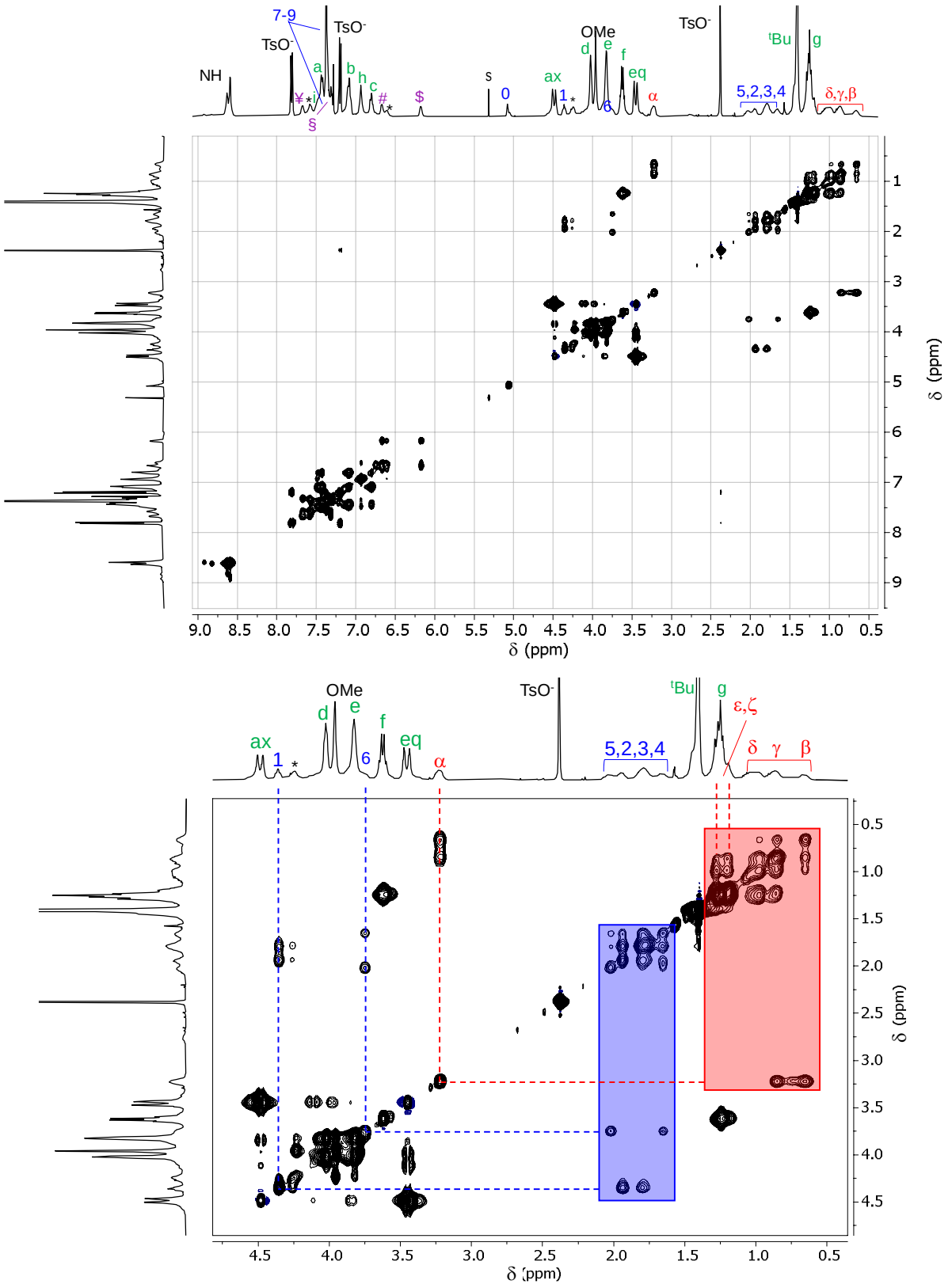

Figure S5. (Top) 2D TOCSY spectrum of $R6_{UU}$ ($CDCl_3$, 400 MHz, mixing time = 40 ms); (down) mid-high fields expansion: the red rectangle highlights the signals of the inner spacer, the blue rectangle those of the external arms.

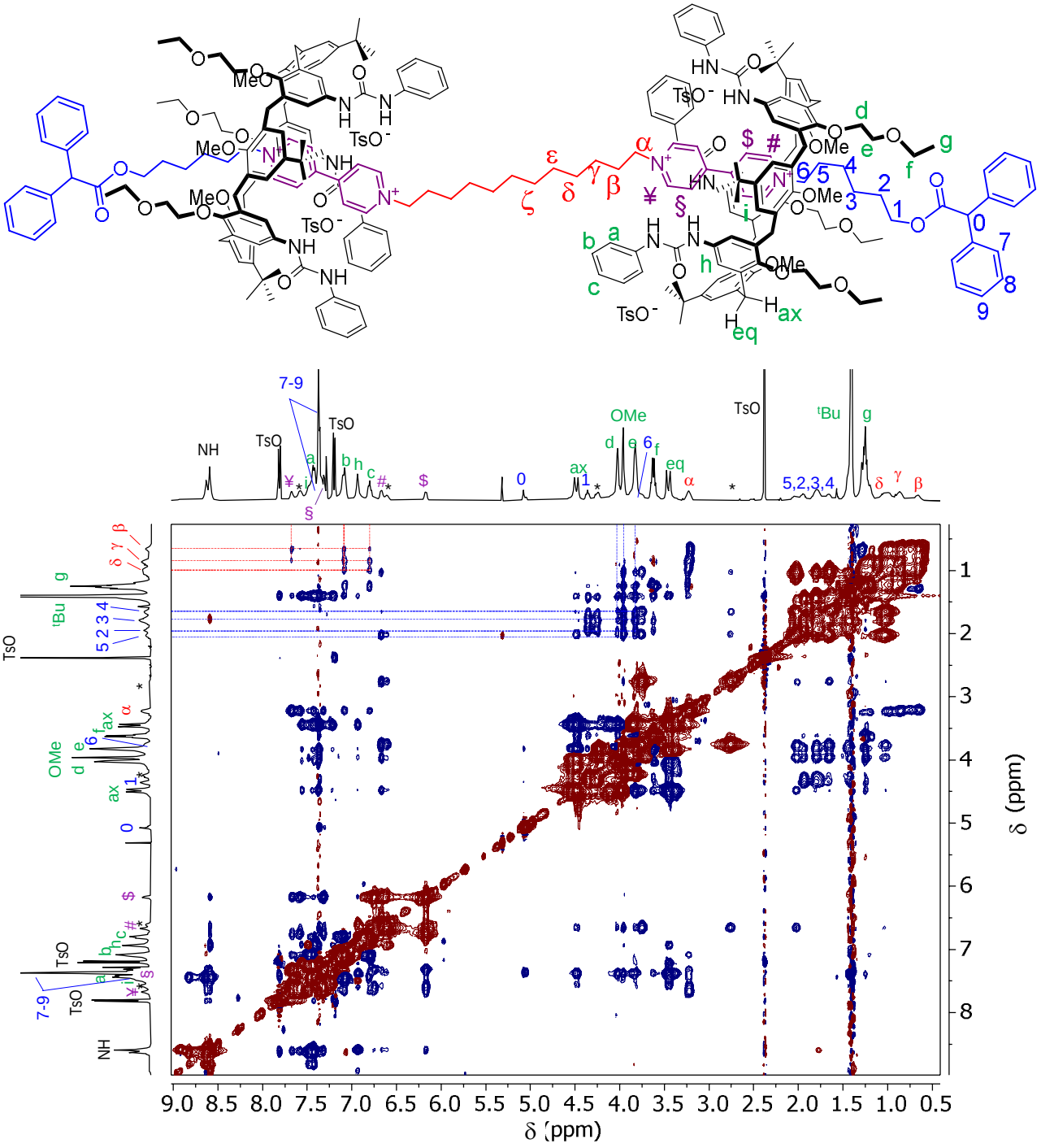

Figure S6. 2D ROESY spectrum of $R6_{UU}$ ($CDCl_3$, 400 MHz, spin-locking = 200 ms). The cross-peaks with blue contours (negative signals) indicate dipolar coupling between protons, while those with reddish contours (positive signals) indicate either diagonal peaks or cross-peaks due to chemical exchange. The red dashed lines indicate the spatial proximity between the inner alkyl spacer, protons *β*–*δ*, and the phenylurea groups at the wheels upper rim, protons *b* and *c*. Blue dashed lines evidence the spatial proximity between the dumbbell external alkyl chains, protons *2*–*5*, and the methoxy (*OMe*) and ethoxyethyl protons (*d* and *e*) present at the wheels lower rim. For the protons labelling, see the sketch above the spectra.

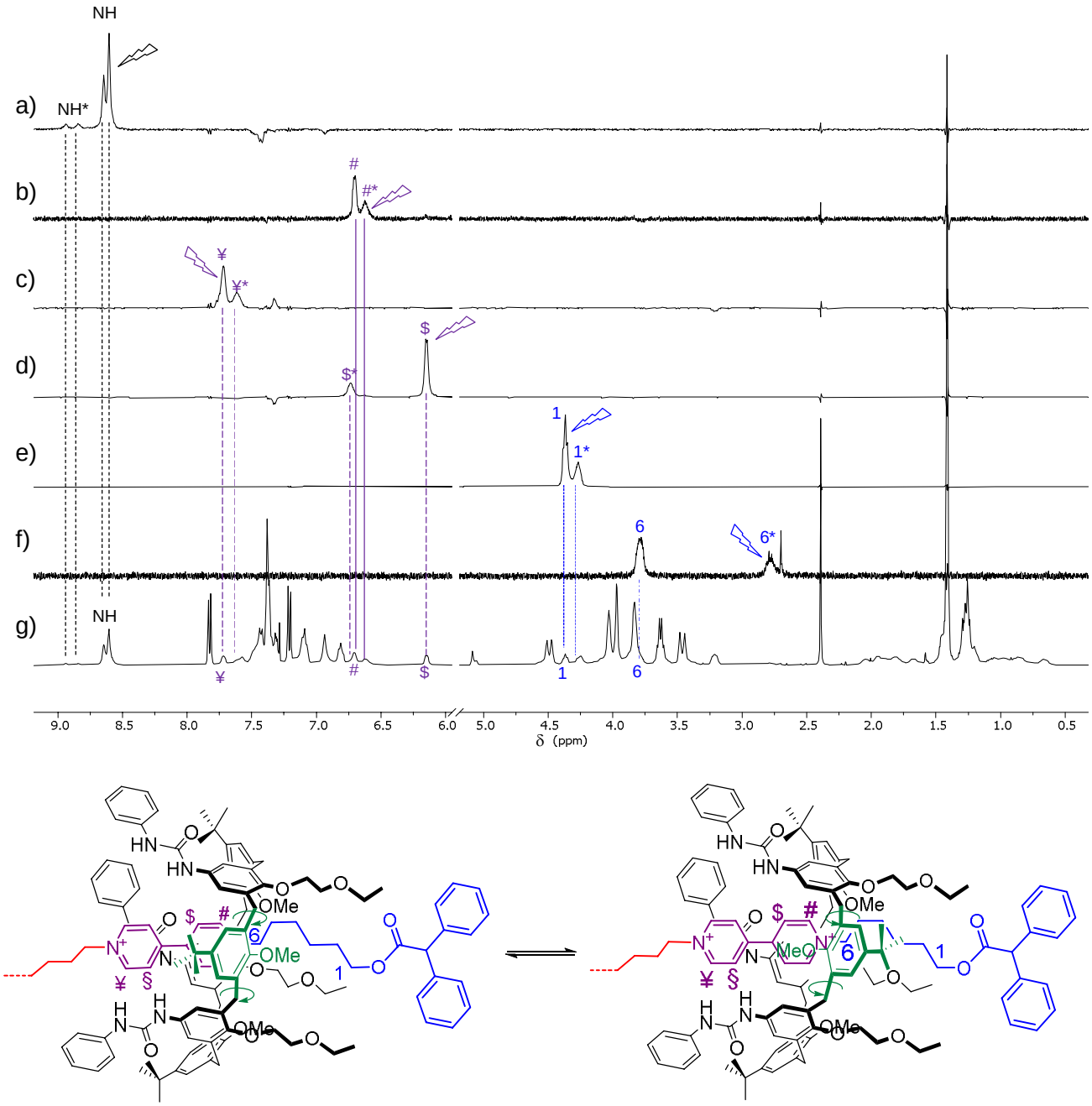

Figure S7 ^{1}H NMR stack plot (400 MHz, $CDCl_3$) of the 1D gradient-selected ROESY spectra of $R6_{UU}$ (spin-lock = 200 ms) obtained by irradiating the following resonances: a) 8.62, b) 6.62, c) 7.72, d) 6.14, e) 4.37, f) 2.78 ppm, and g) non-irradiated spectrum of $R6_{UU}$ taken as the reference. The positive peaks indicate the resonances in chemical exchange with the irradiated ones, while the negative peaks are due to dipolar coupling. Note that more than one positive peak is present in spectrum c) because of the overlap of the ¥ resonance with other wheel's signals. Spectrum f) was recorded using a 1D gradient-selected NOESY sequence for sensitivity reasons. The sketch below the stack plot shows the possible flip of one of the p-*tert*-butyl anisole ring of the wheel (coloured in dark green) in the *cone* conformation (left) that determines the *paCo* rotamer formation (right). To evaluate as the *paCo* rotamer's formation affects the wheel's signals, see the asterisked correlations in the HSQC depicted in Fig. S3.

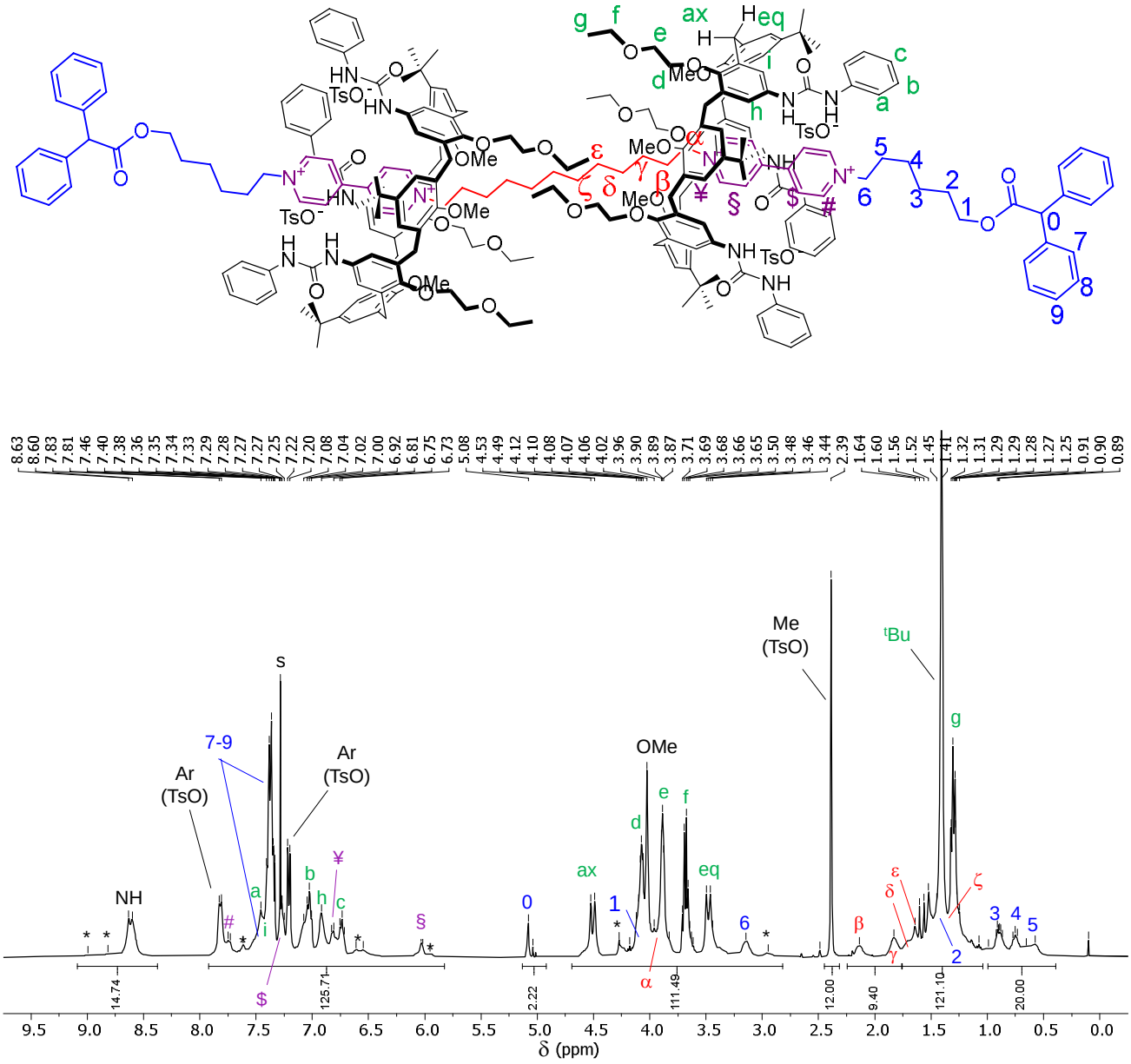

Figure S8. ^{1}H NMR spectrum (400 MHz, $CDCl_3$) of [3]rotaxane $R6_{LL}$. The signals deriving from the *paCo* rotamer are indicated with an asterisk.

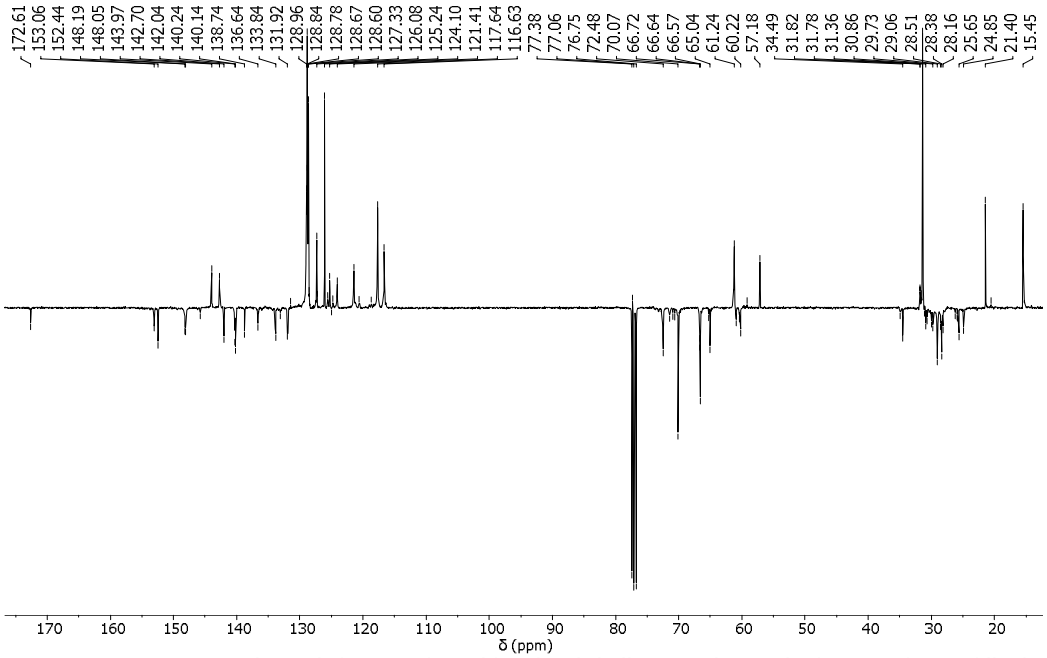

Figure S9. ^{13}C DEPT-Q spectrum of $R6_{LL}$ in $CDCl_3$ (100 MHz). Positive signals indicate tertiary and primary carbons while the negative the quaternary and secondary ones (solvent signals are negative).

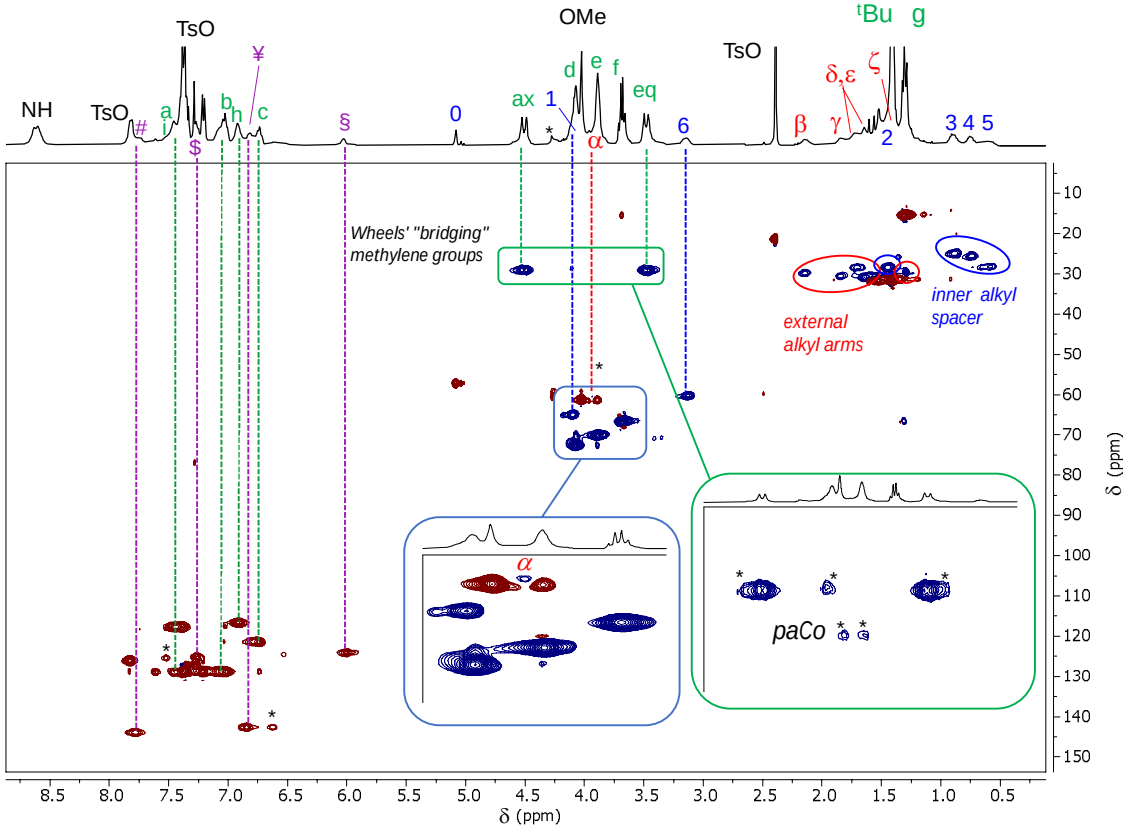

Figure S10. 2D edited HSQC spectrum of [3]rotaxane $R6_{LL}$. The cross-peaks with blue contours indicate CH couplings of tertiary and primary carbons, while those with reddish contours the CH couplings of secondary carbons. The cross-peaks relative to the macrocycles methylene bridging units have been highlighted with a green box, while those relative to the external and internal alkyl chains with blue and red ellipses, respectively. The inset shows the enhanced correlations of the bridging methylene groups of the *paCo* rotamer (all the projection peaks and correlations arising from this rotamer have been indicated with an asterisk).

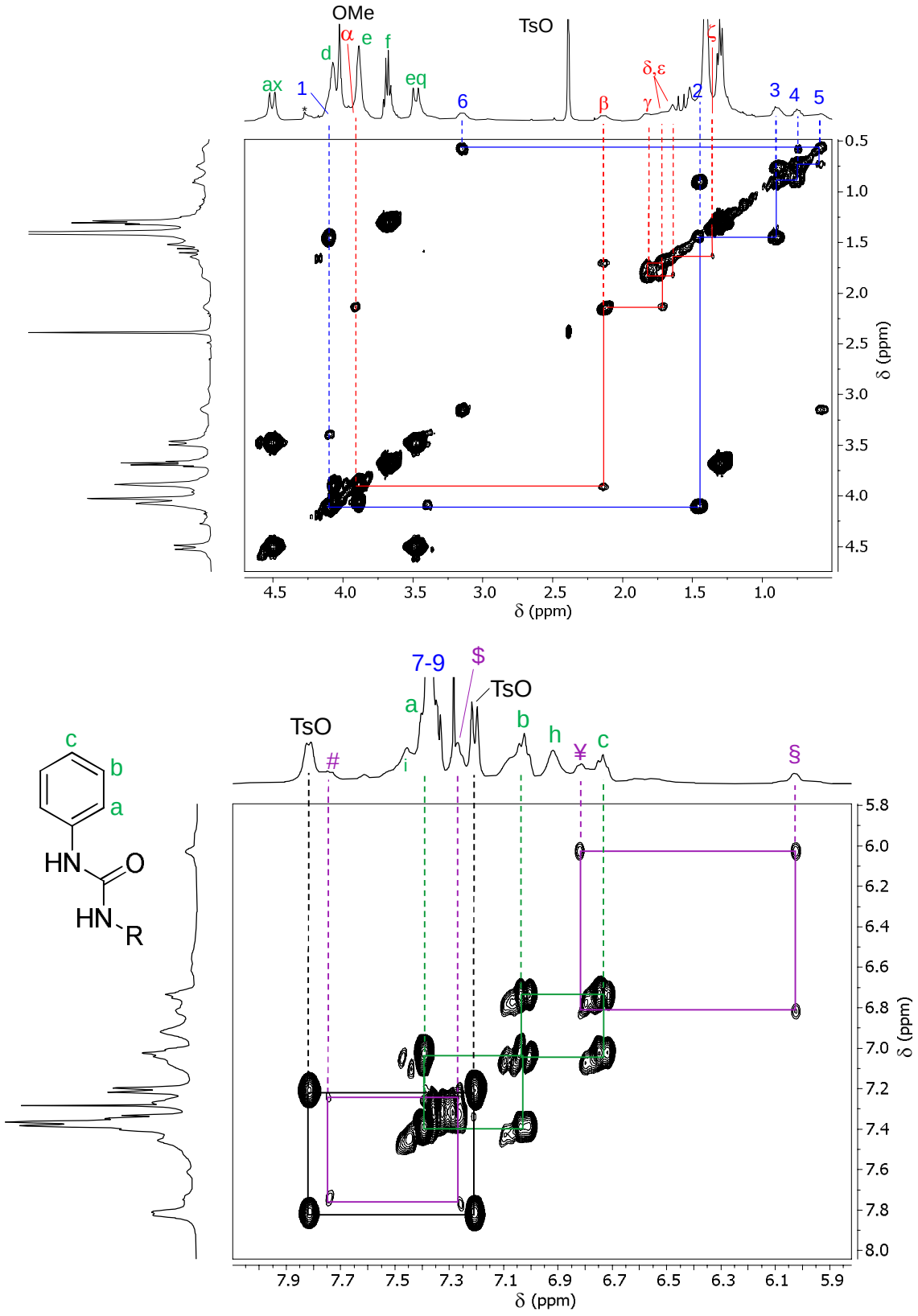

Figure S11. (Top) Mid-high and (down) low fields expansions of magnitude mode DQF-COSY of $R6_{LL}$ ($CDCl_3$, 400 MHz).

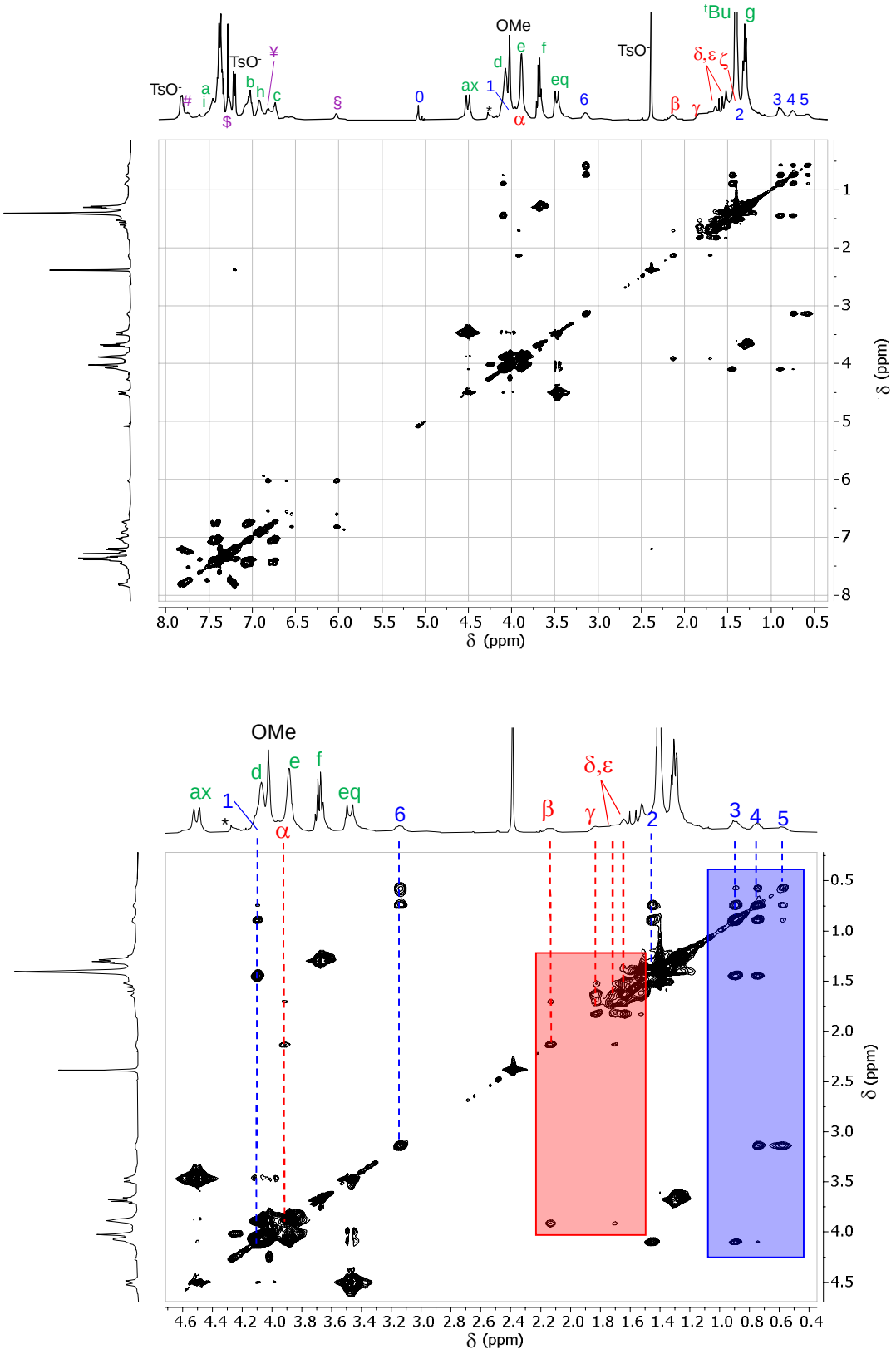

Figure S12. (Top) 2D TOCSY spectrum of $R6_{LL}$ ($CDCl_3$, 400 MHz, mixing time = 40 ms); (down) mid-high fields expansion: the red rectangle highlights the signals of the inner spacer, the blue rectangle those of the external arms.

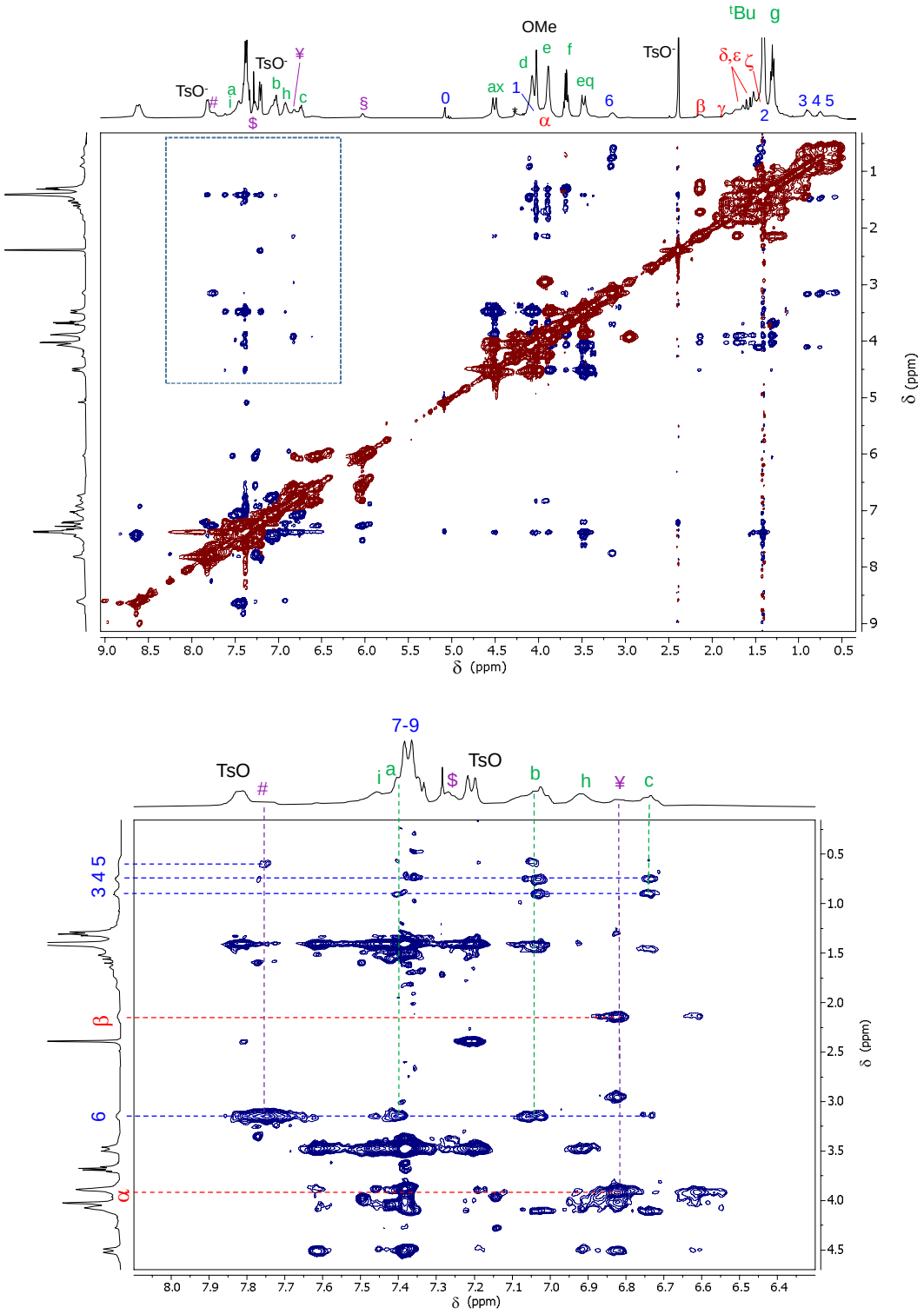

Figure S13. (Top) 2D ROESY spectrum of $R6_{UU}$ ($CDCl_3$, 400 MHz, spin-locking = 200 ms). The cross-peaks with blue contours (negative signals) indicate dipolar coupling between protons, while those with reddish contours (positive signals) indicate either diagonal peaks or cross-peaks due to chemical exchange. (Down) Levels-enhanced expanded region (see dashed box) of the 2D ROESY showing the dipolar coupling between the dumbbell bis-viologen core protons with several wheels' comparts (see the sketch of the following page for further details); for the sake of clarity, only negative levels are presented.

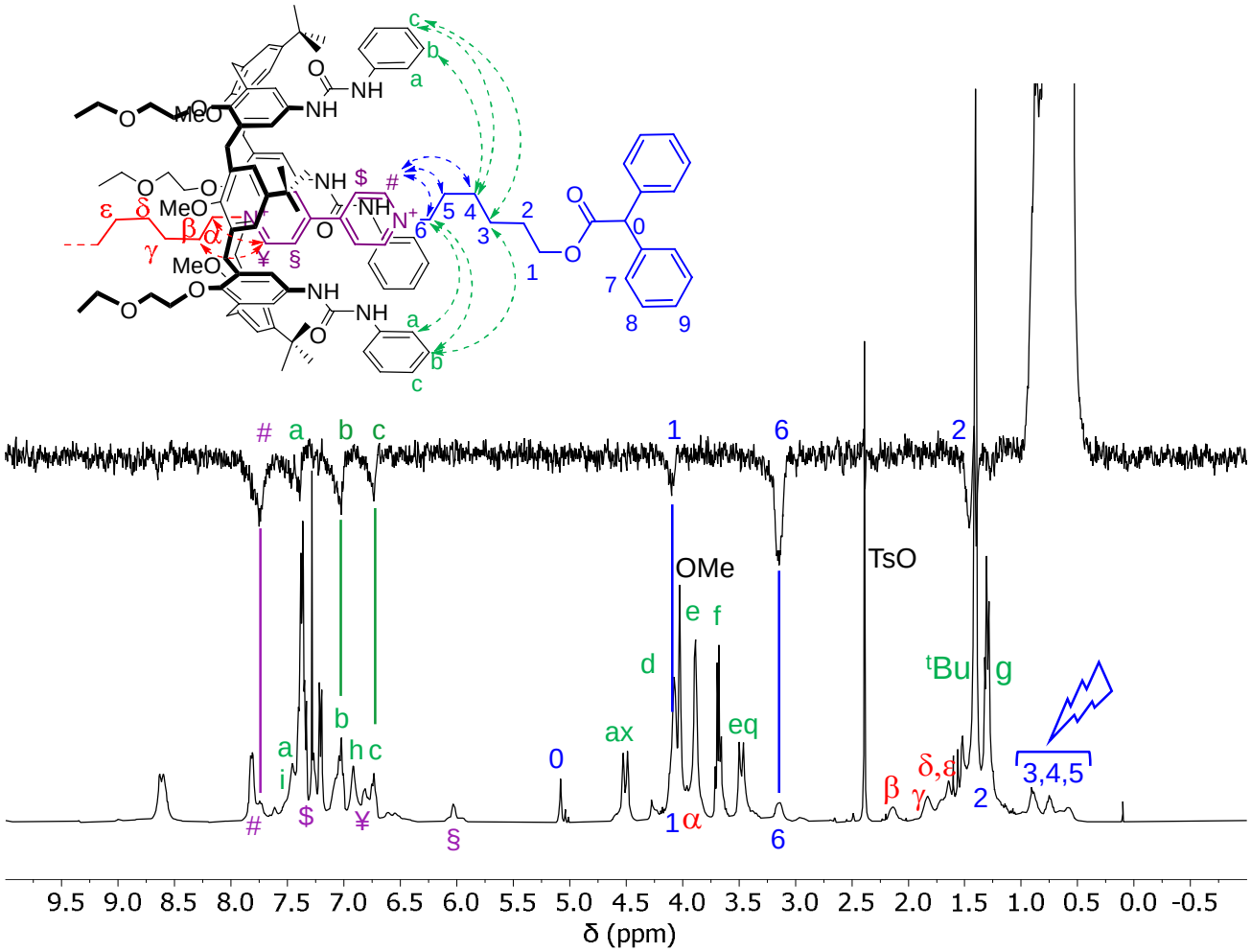

Figure S14 1D selective ROESY spectrum (400 MHz, SL = 200 ms) with PFG signal selection of protons 3,4,5 (0.66 ppm); (bottom) the ^{1}H NMR reference spectrum. The protons spatial proximity has been highlighted with purple, green and blue solid lines (see the sketch above the stack for the protons labelling).

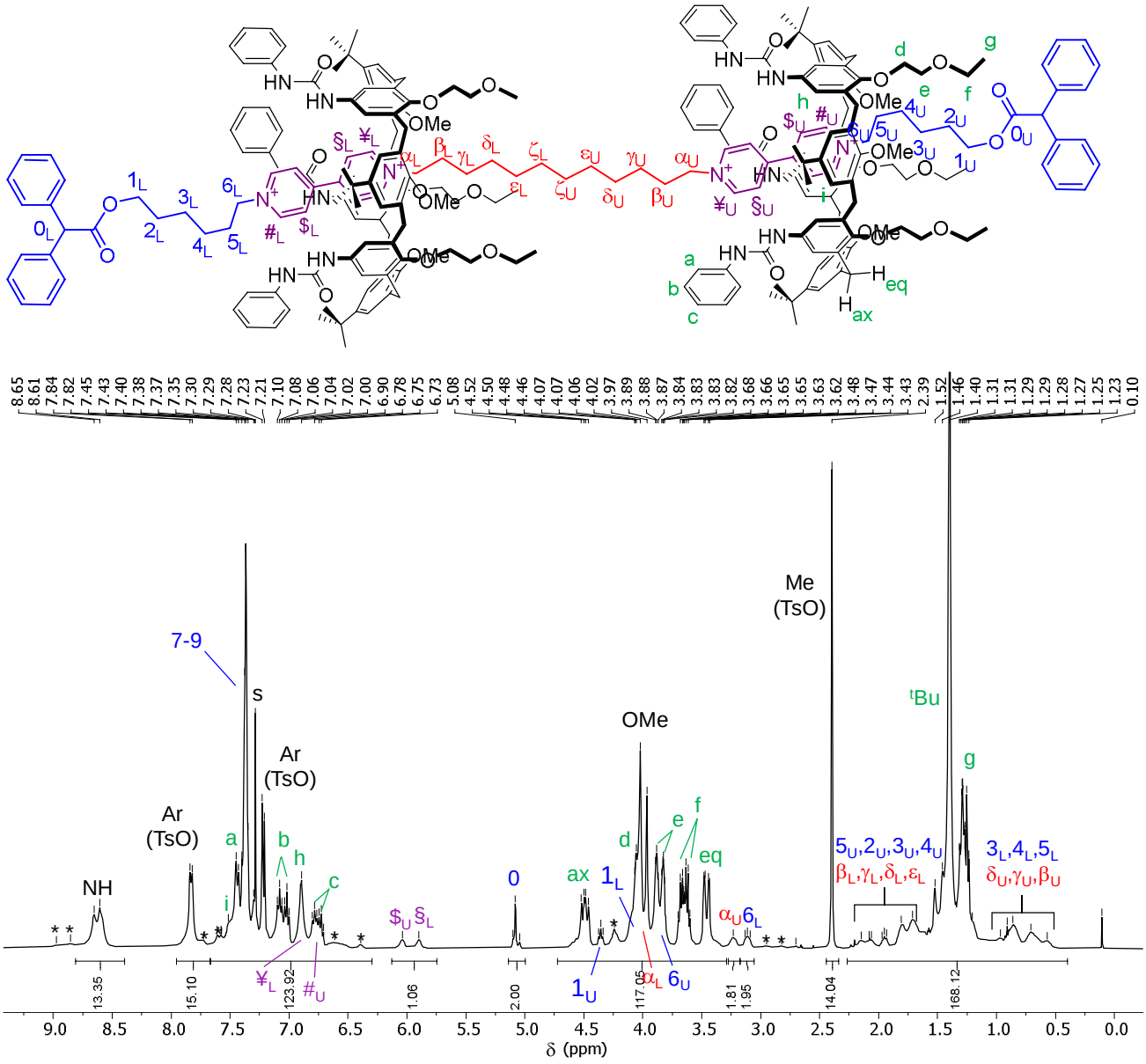

Figure S15. ^{1}H NMR spectrum (400 MHz, $CDCl_3$) of [3]rotaxane $R6_{UL}$. Signals of the wheels' *paCo* rotamers are indicated with asterisks.

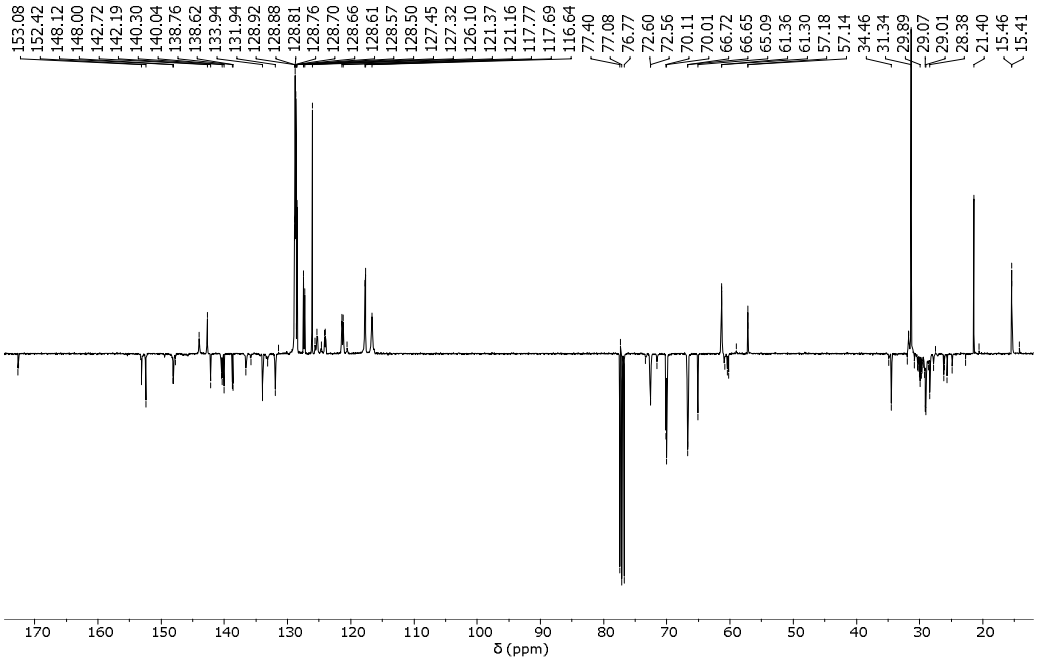

Figure S16. ^{13}C DEPT-Q spectrum of $R6_{UL}$ in $CDCl_3$ (100 MHz). Positive signals indicate tertiary and primary carbons while the negative the quaternary and secondary ones (solvent signals are negative).

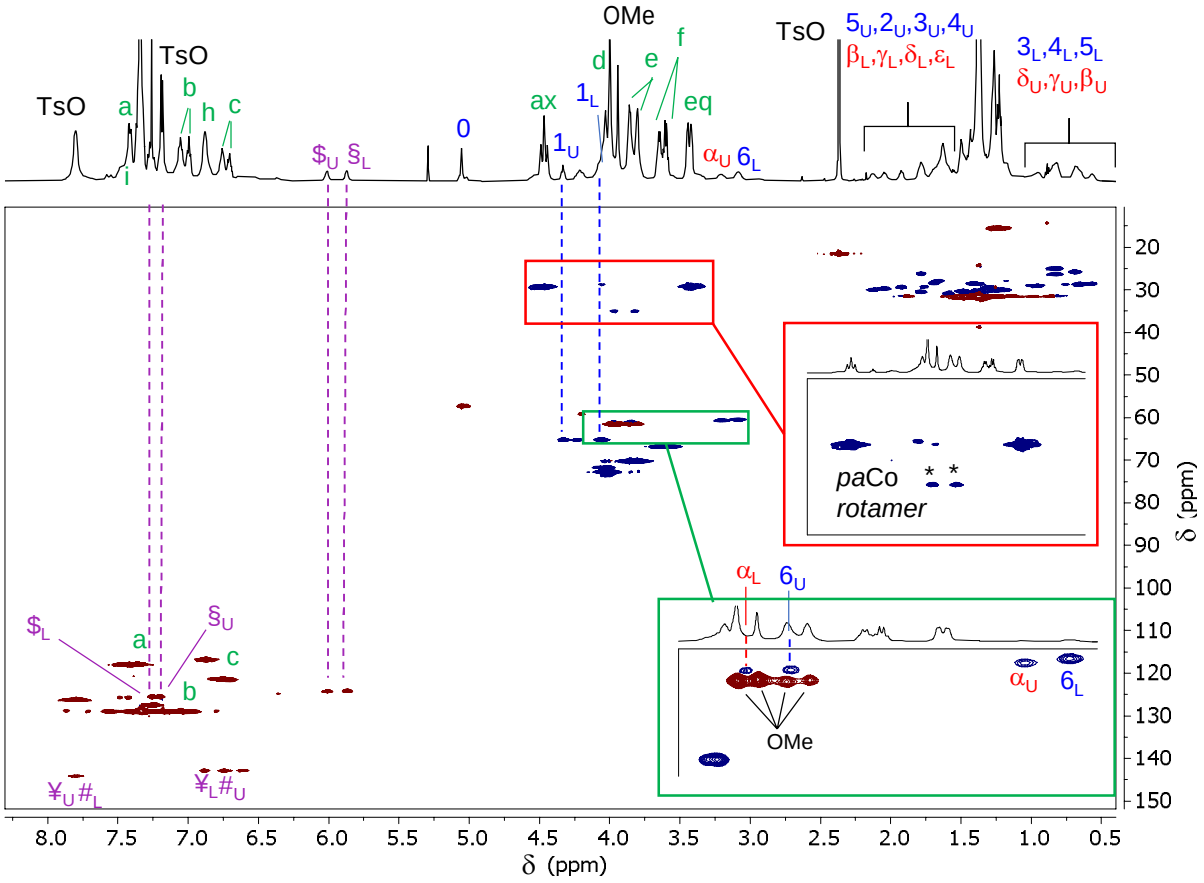

Figure S17. ^{1}H-^{13}C edited HSQC NMR spectrum of $R6_{UL}$ in $CDCl_3$ (600 MHz for ^{1}H, 298 K). The methylene groups' cross-peaks have blue contours, while those of methine and methyl groups red contours.

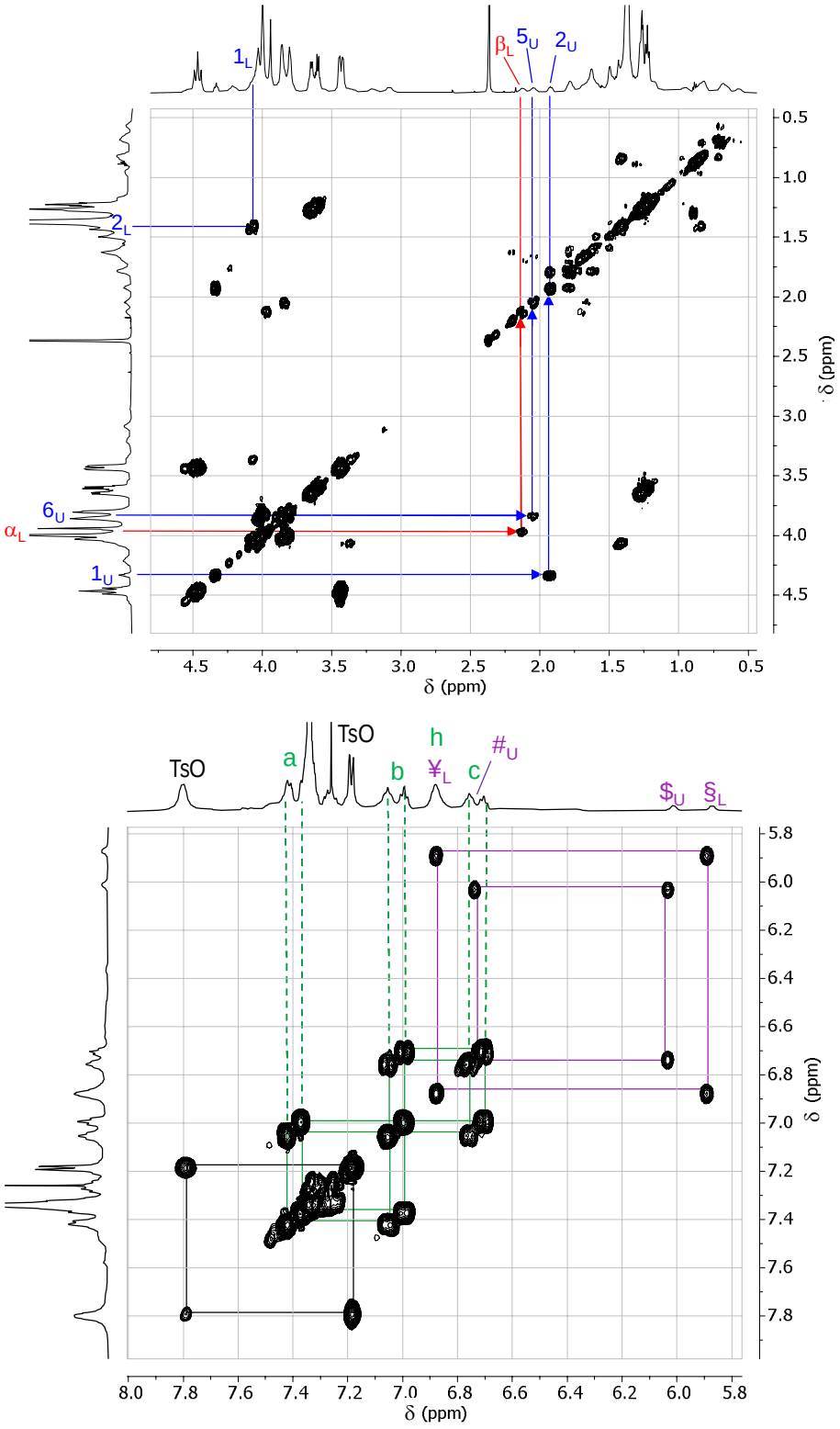

Figure S18. (Top) Mid-high and (down) low-fields expansions of a magnitude mode DQF-COSY of $R6_{UL}$ ($CDCl_3$, 600 MHz). The red lines highlight the inner spacer's cross-peaks, the blue lines those of the external arms, the purple lines those of the viologen units, the green lines those of phenylureido groups of CX.

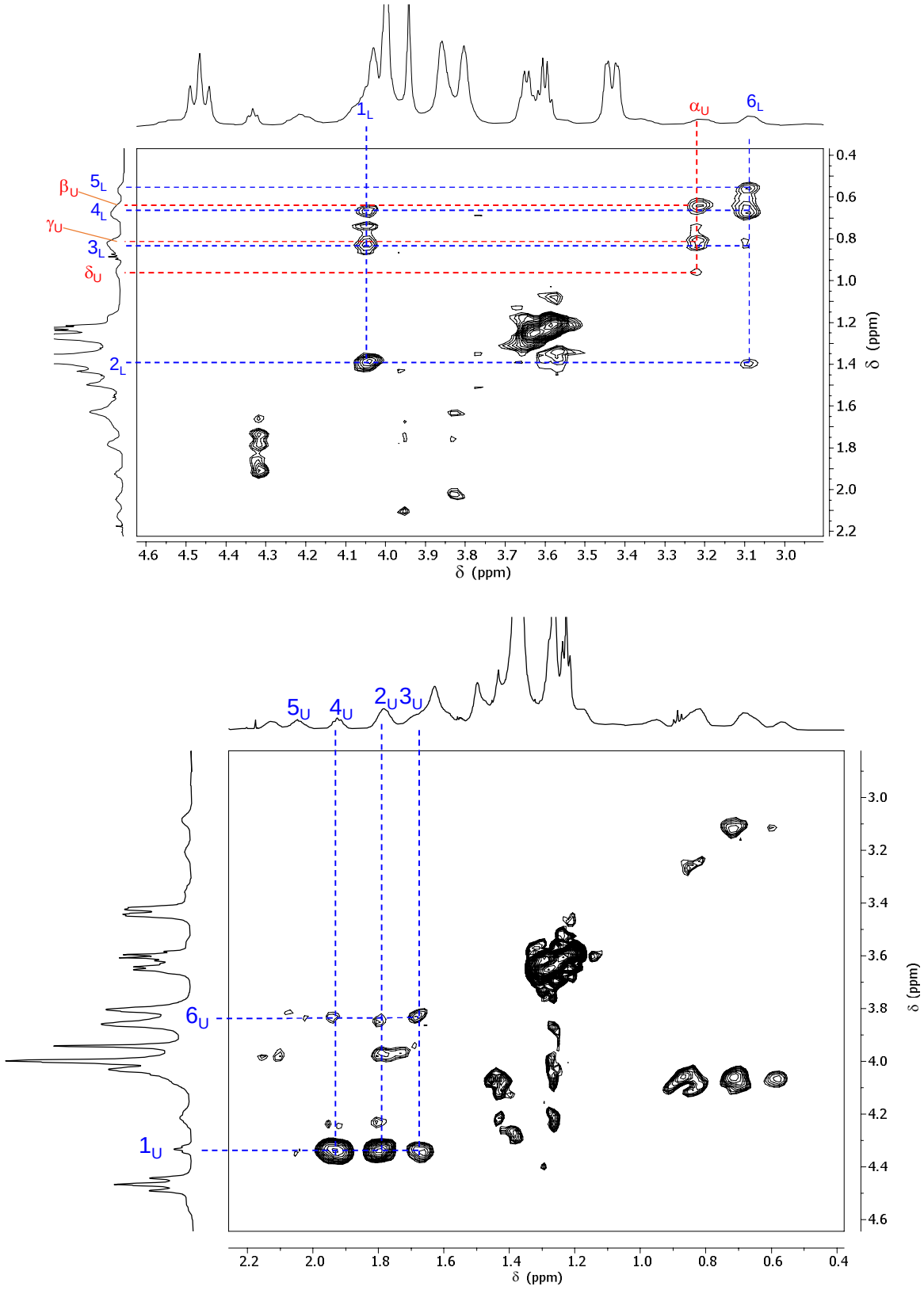

Figure S19. (Top) Mid and (down) high fields expansions of the 2D TOCSY spectrum of $R6_{UL}$ ($CDCl_3$, 600 MHz, 298 K, mixing time = 60 ms). The red lines highlight the inner spacer's cross-peaks, the blue lines those of the external arms.

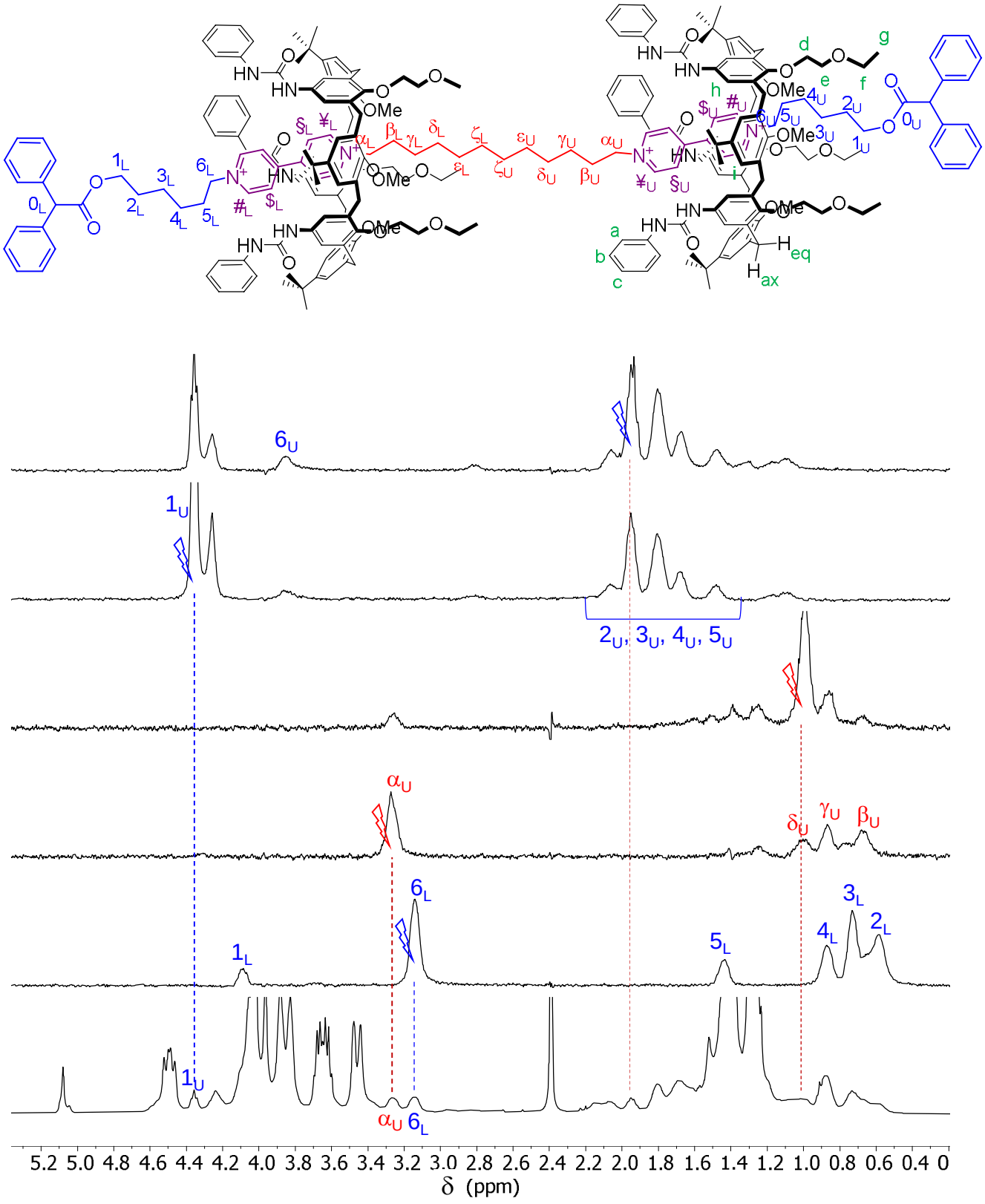

Figure S20. Stack plot ($CDCl_3$, 600 MHz) of 1D selective TOCSY spectra (mixing time: 0.06 s) with several PFG signal selection. The ^1H NMR reference spectrum of $R6_{UL}$ is at the bottom of the stack.

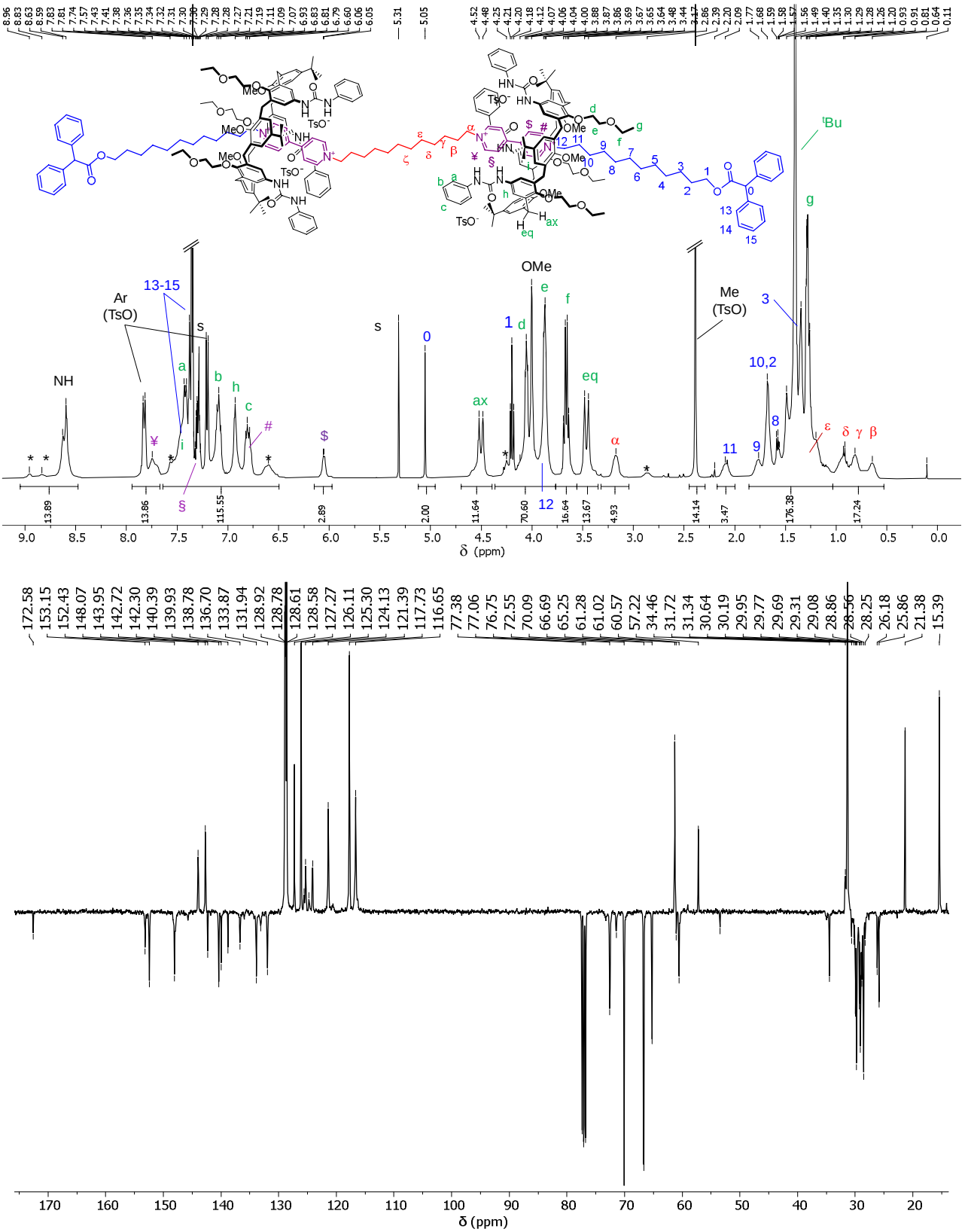

Figure S21. (Top) ^{1}H (400 MHz, $CDCl_3$) and (down) ^{13}C DEPT-Q (100 MHz, $CDCl_3$) spectra of $R12_{UU}$. The asterisks in the proton spectrum indicate the resonances assigned to the wheel's *paCo* rotamer (see Fig. S7). In the DEPT-Q spectrum, the signals relative to primary and tertiary carbons are phased positive, while secondary and quaternary carbons are negative.

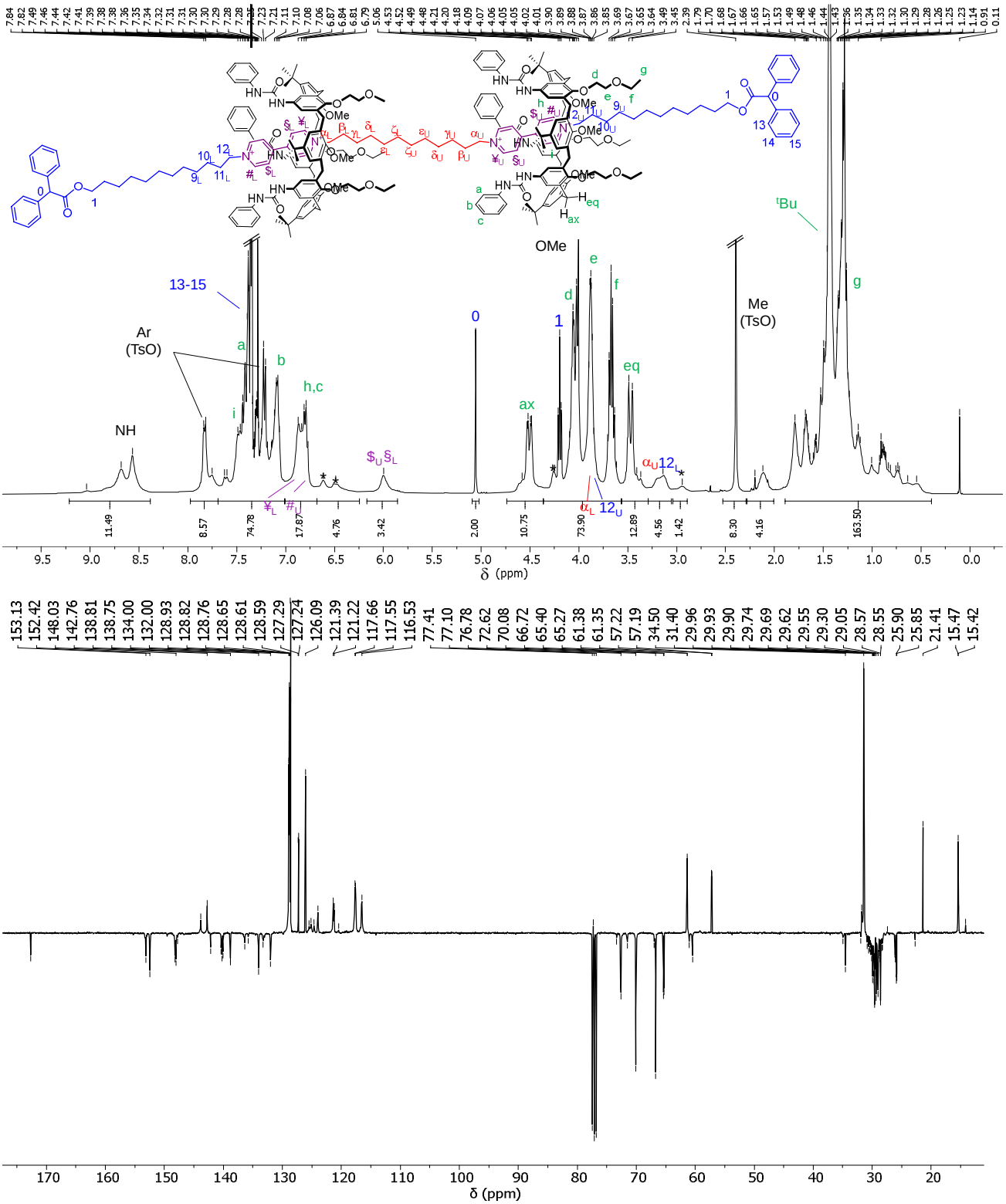

Figure S22. (Top) ^{1}H (400 MHz, $CDCl_3$) and (down) ^{13}C DEPT-Q (100 MHz, $CDCl_3$) spectra of $R12_{UL}$. The asterisks in the proton spectrum indicate the resonances assigned to the wheel's *paCo* rotamer (see Fig. S7). In the DEPT-Q spectrum, the signals relative to primary and tertiary carbons are phased positive, while secondary and quaternary carbons are negative.

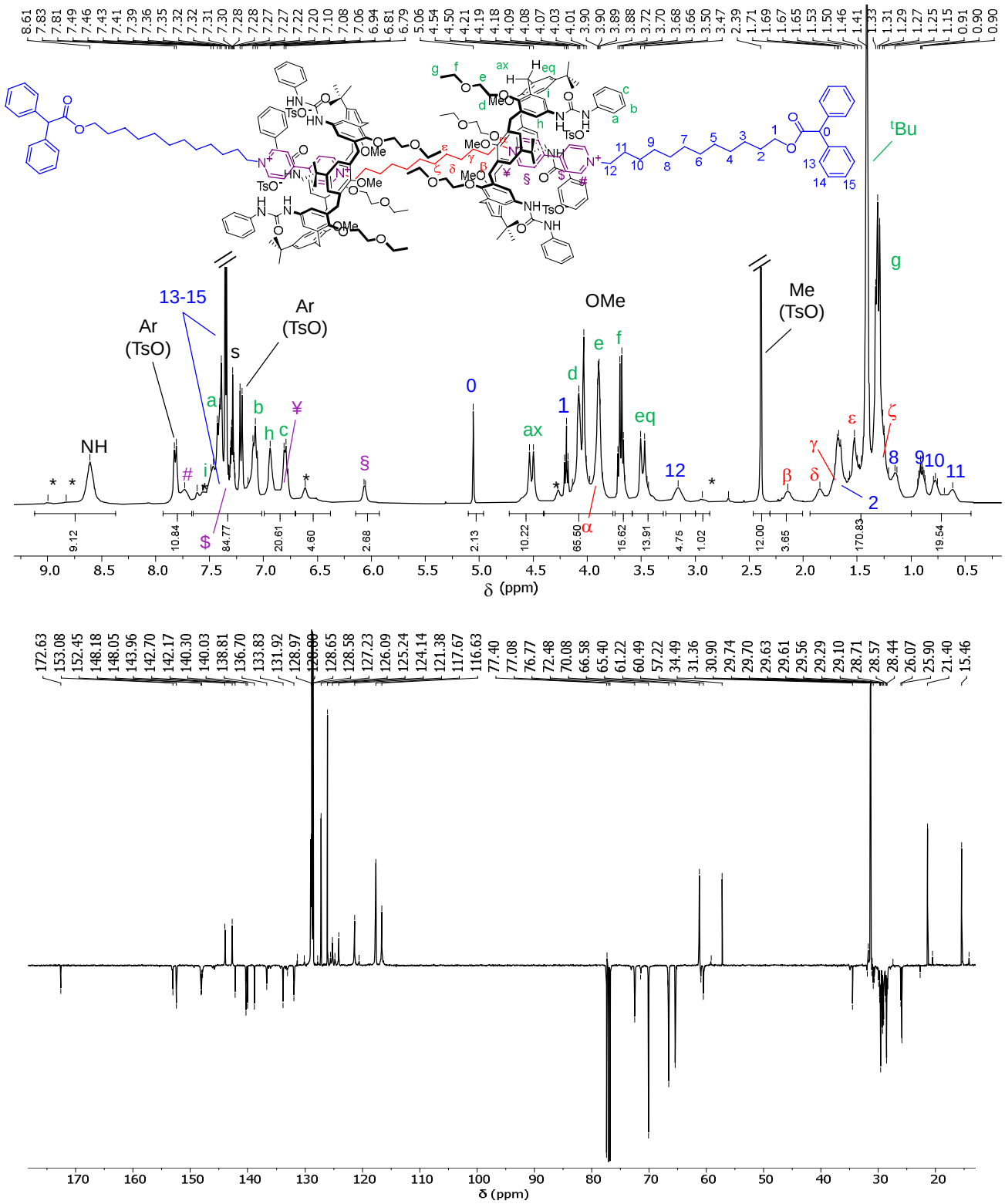

Figure S23. (Top) ^{1}H (400 MHz, $CDCl_3$) and (down) ^{13}C DEPT-Q (100 MHz, $CDCl_3$) spectra of $R12_{LL}$. The asterisks in the proton spectrum indicate the resonances assigned to the wheel's *paCo* rotamer (see Fig. S7). In the DEPT-Q spectrum, the signals relative to primary and tertiary carbons are phased positive, while secondary and quaternary carbons are negative.

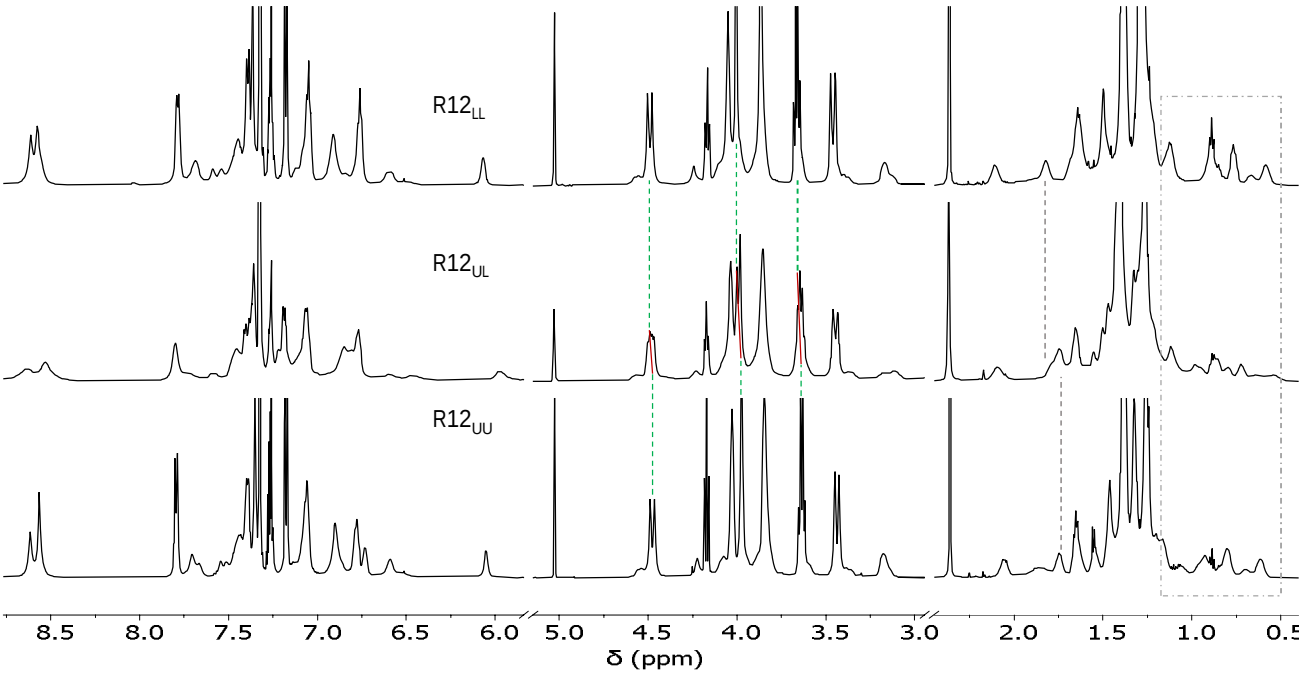

Figure S24 ^{1}H NMR stack plot (600 MHz, $CDCl_3$) of the oriented [3]rotaxanes $R12_{UU}$ (bottom), $R12_{UL}$ (middle) and $R12_{LL}$ (top).

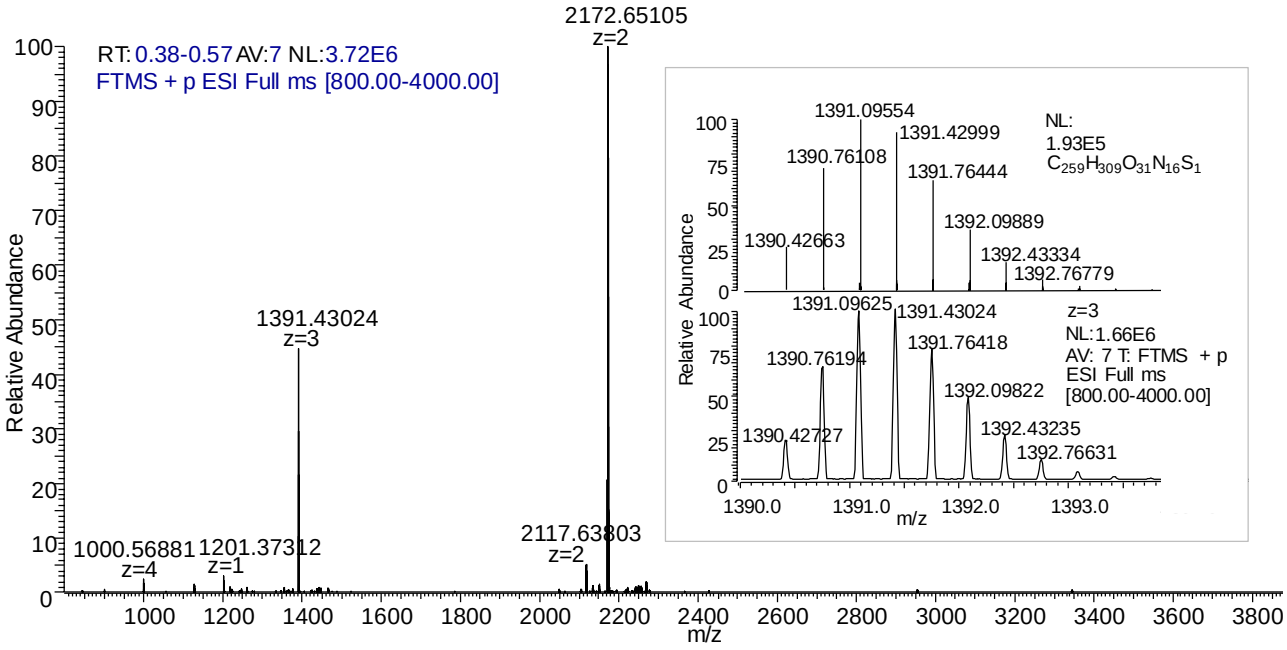

Figure S25. HR-MS spectra of $R6_{UU}$; in the inset, the experimental isotopic distribution is compared with the calculated one.

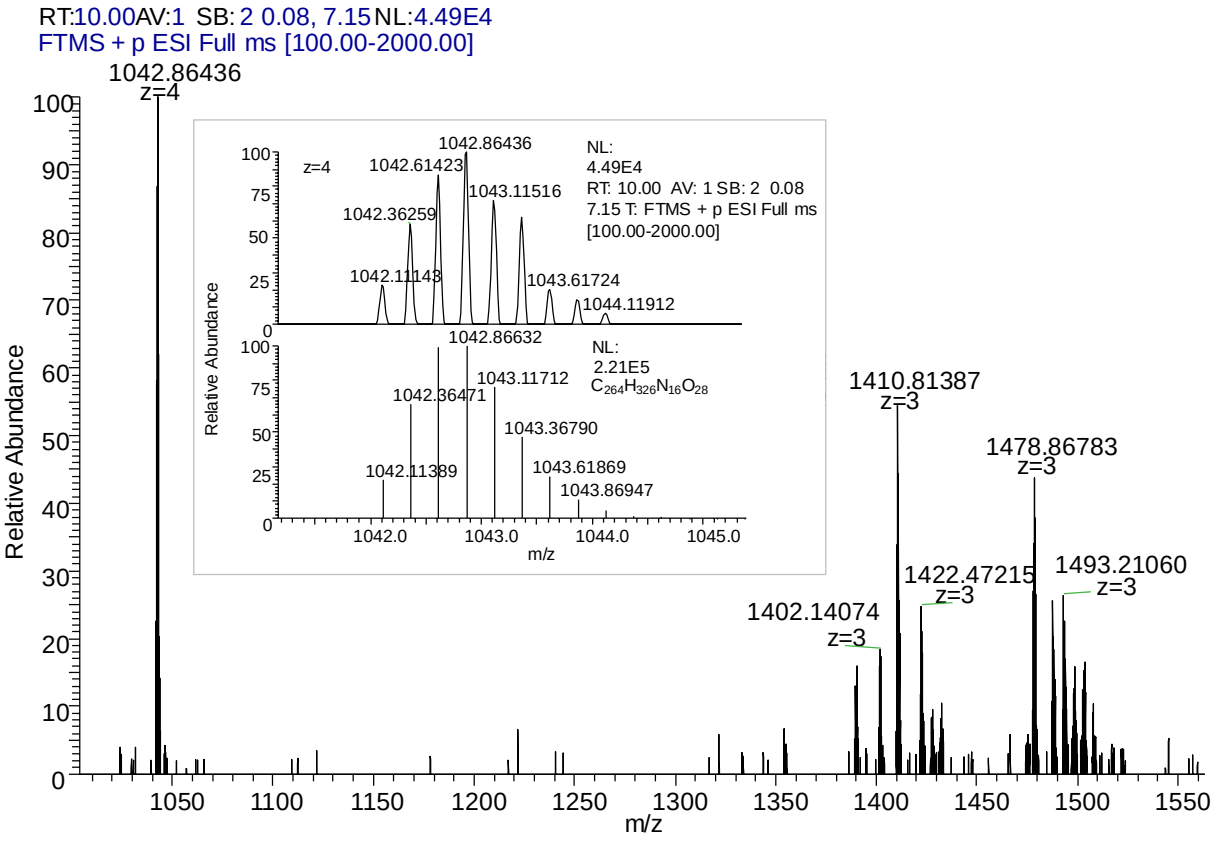

Figure S26 HR-MS spectra of $R12_{UU}$; in the inset, the experimental isotopic distribution is compared with the calculated one.

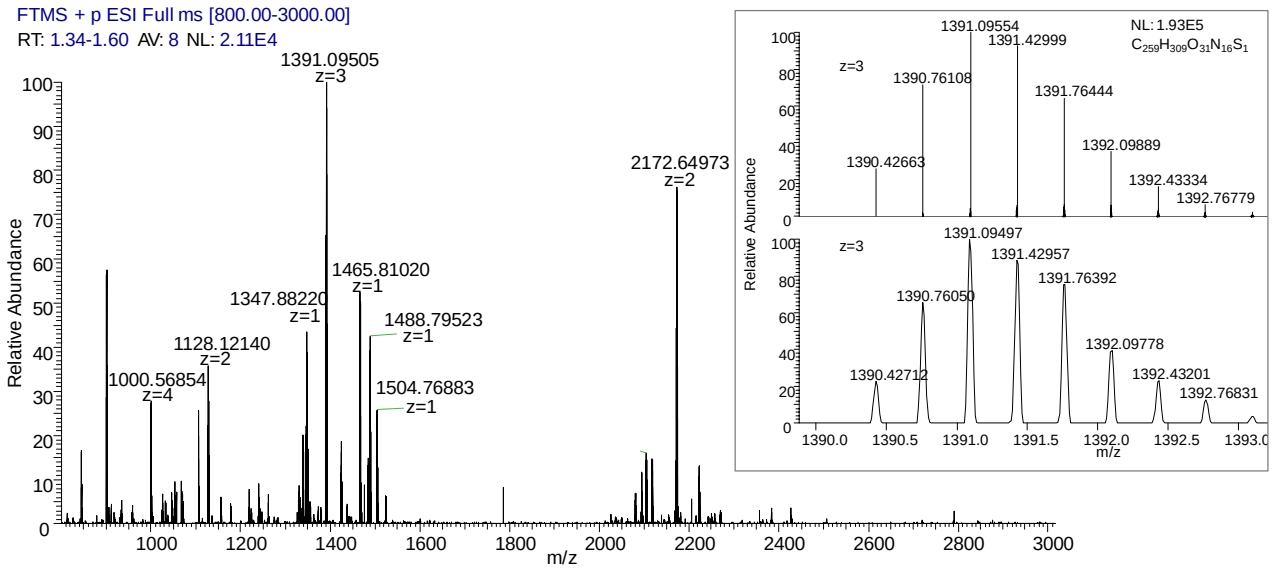

Figure S27. HR-MS spectra of $R6_{LL}$, in the inset, the experimental isotopic distribution is compared with the calculated one.

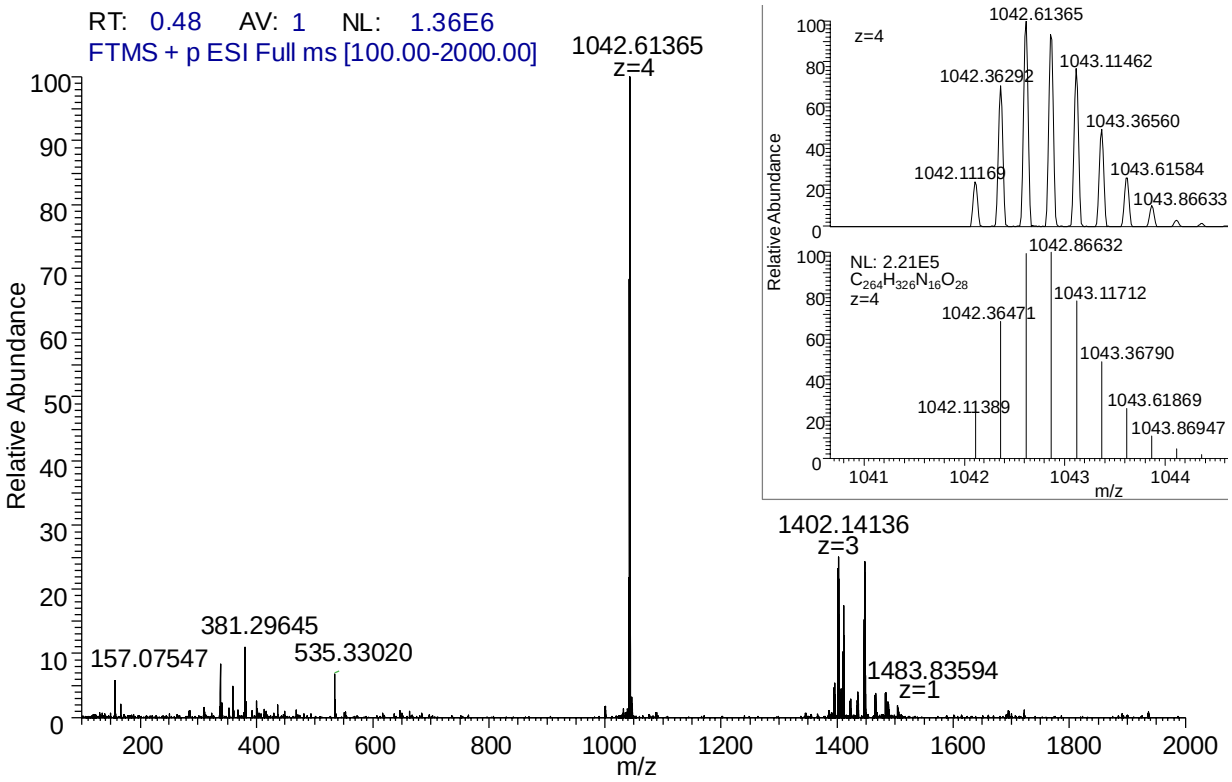

Figure S28. HR-MS spectra of $R12_{LL}$, in the inset, the experimental isotopic distribution is compared with the calculated one.

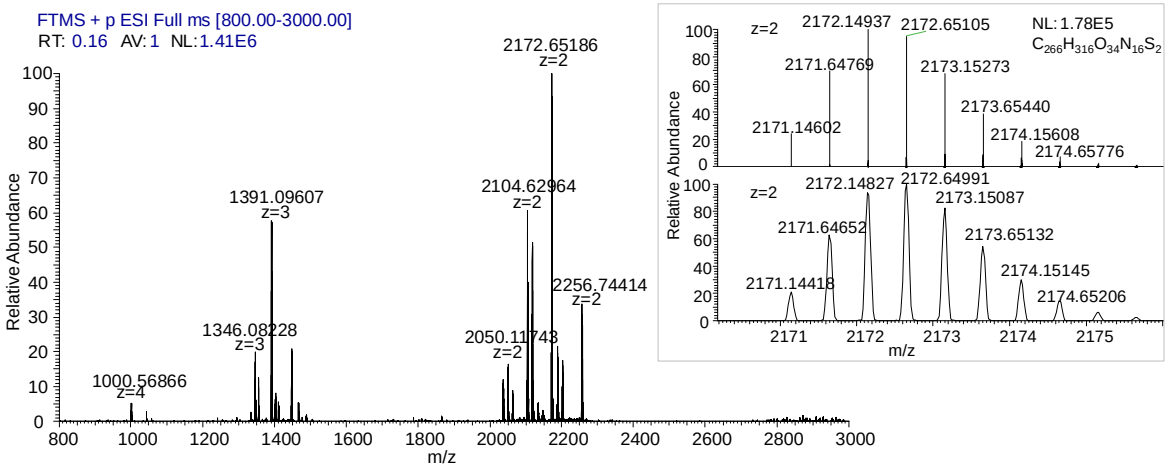

Figure S29. HR-MS spectra of $R6_{UL}$, in the inset, the experimental isotopic distribution is compared with the calculated one.

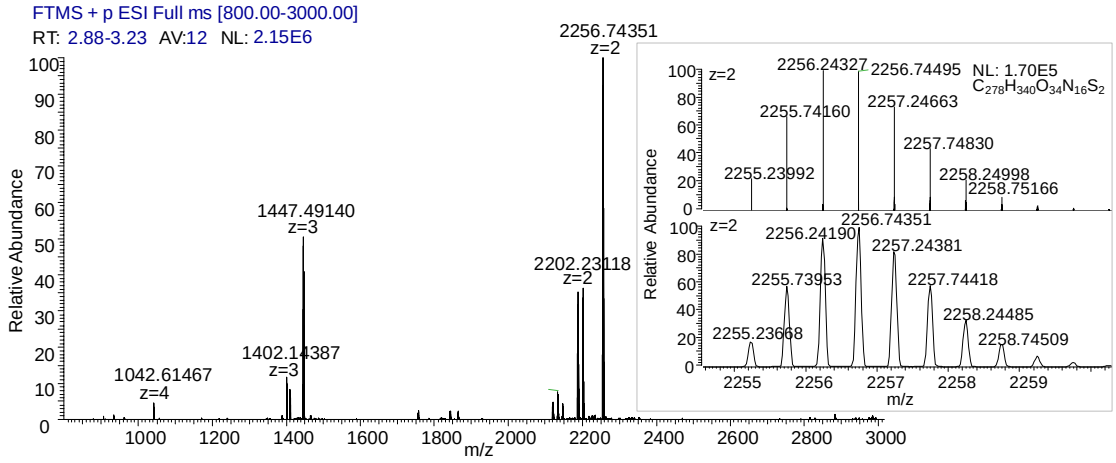

Figure S30. HR-MS spectra of $R12_{UL}$, in the inset, the experimental isotopic distribution is compared with the calculated one.

Table S1. Photophysical data of the investigated species in CH_2Cl_2 at room temperature. (a) The number of independent measurements is indicated in parentheses. (b) The absorption coefficient could not be precisely determined because of the low solubility in CH_2Cl_2.

Species	λ_{max} (nm)	ε [a] (M^{-1} cm^{-1})
$R6_{UU}$	258	196800 ± 6900 (2)
$R6_{LL}$	259	201900 ± 3700 (3)
$R6_{UL}$	259	197600 ± 4400 (2)
$R12_{UU}$	259	187600 ± 6500 (3)
$R12_{LL}$	259	185100 ± 6000 (3)
$R12_{UL}$	259	186000 ± 6500 (3)
Dumbbell 7a	267	[b]
Dumbbell 7b	267	[b]

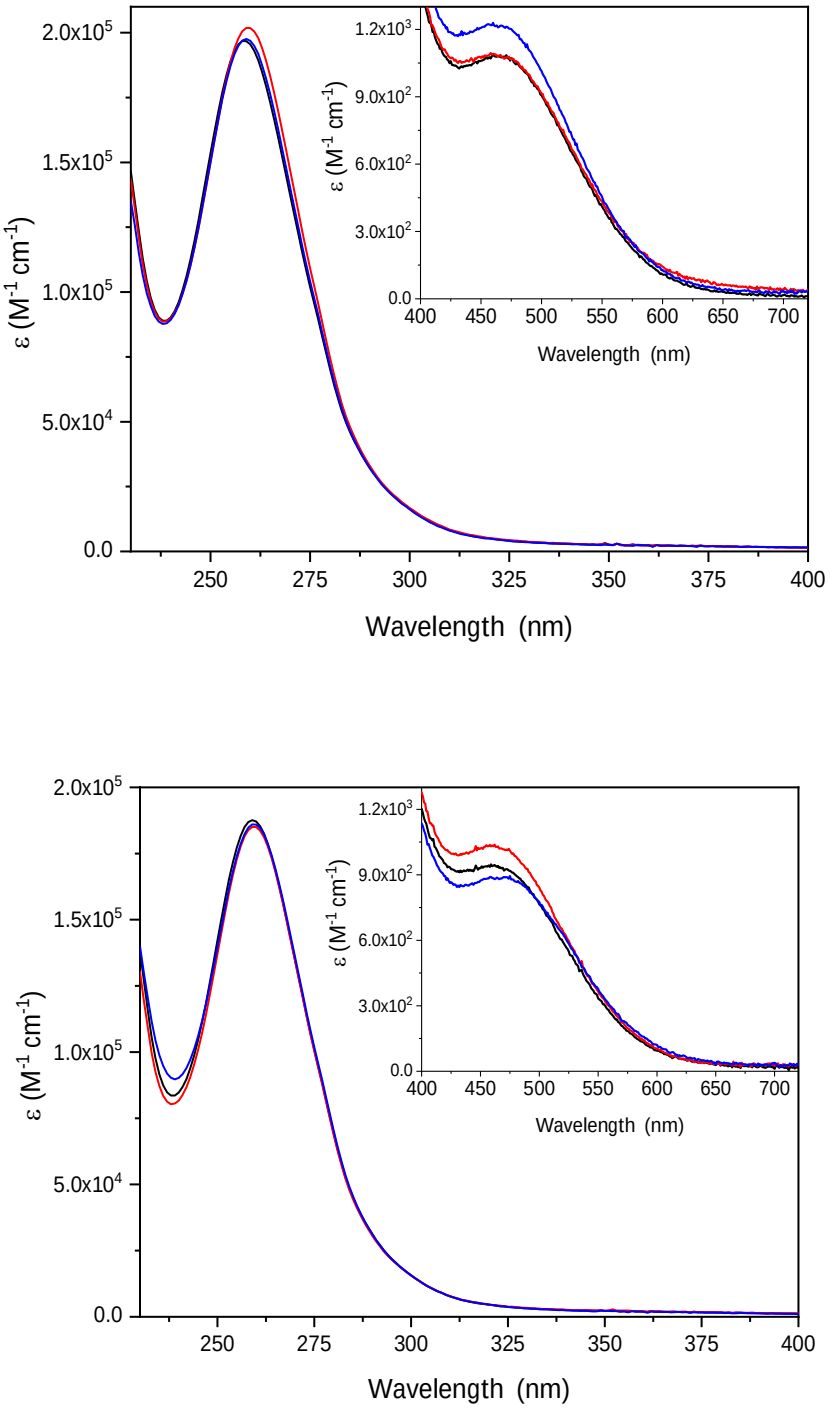

Figure S31. (Top) Absorption spectra of the [3]rotaxanes $R6_{UU}$ (Black), $R6_{LL}$ (Red) and $R6_{UL}$ (Blue) in CH_2Cl_2. Inset: Charge-transfer absorption bands of the [3]rotaxanes. (Bottom) Absorption spectra of the [3]rotaxanes $R12_{UU}$ (Black), $R12_{LL}$ (Red) and $R12_{UL}$ (Blue) in CH_2Cl_2. Inset: Charge-transfer absorption bands of the [3]rotaxanes.

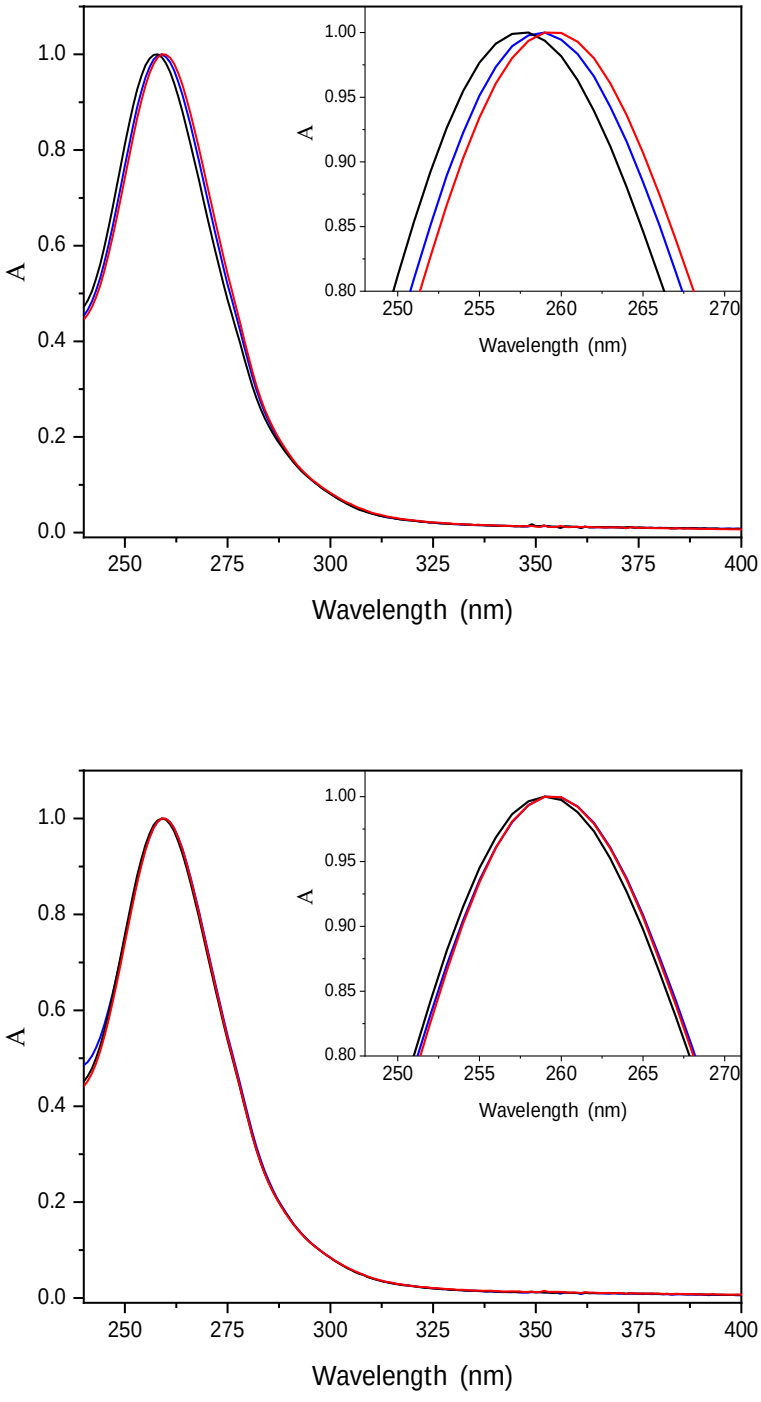

Figure S32. (Top) Absorption spectra of the [3]rotaxanes $R6_{UU}$ (Black), $R6_{LL}$ (Red) and $R6_{UL}$ (Blue) in CH_2Cl_2. The spectra are normalised with respect to the maximum absorption. Inset: Maximum of the absorption bands of the [3]rotaxanes. (Bottom) Absorption spectra of the [3]rotaxanes $R12_{UU}$ (Black), $R12_{LL}$ (Red) and $R12_{UL}$ (Blue) in CH_2Cl_2. The spectra are normalised with respect to the maximum of absorption. Inset: Maximum of the absorption bands of the [3]rotaxanes.

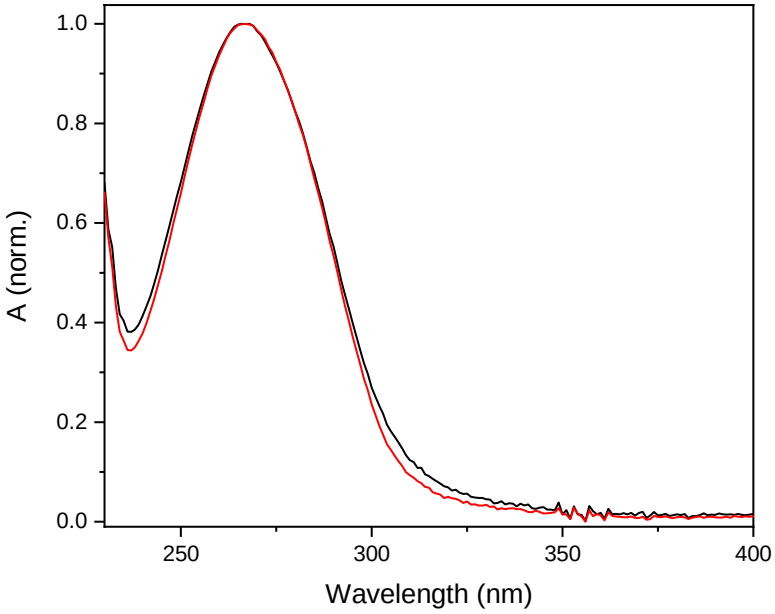

Figure S33. Absorption spectra of the dumbbells 7a (Black) and 7b (Red) in CH_2Cl_2. The spectra are normalised with respect to the maximum of absorption.

Table S2. Electrochemical potentials of the investigated species obtained from the Differential Pulse Voltammetries in CH_2Cl_2.

Species	Reduction potentials (V vs SCE)	
	E_1	E_2
$R6_{UU}$	-0.74	-1.20
$R6_{LL}$	-0.74	-1.19
$R6_{UL}$	-0.72	-1.19
$R12_{UU}$	-0.74	-1.20
$R12_{LL}$	-0.74	-1.20
$R12_{UL}$	-0.75	-1.21
Dumbbell 7a	-0.32	-0.86
Dumbbell 7b	-0.30	-0.85

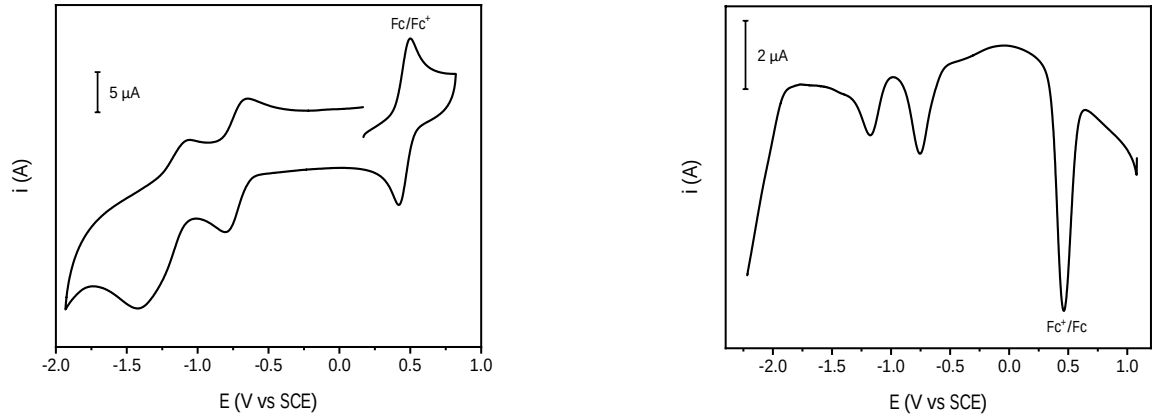

Figure S34. CV (left, scan rate: 200 mV s^{-1}) and DPV (right, scan rate: 20 mV s^{-1}) of a 1.9 × 10^{-4} M solution of $R6_{UU}$ in CH_2Cl_2.

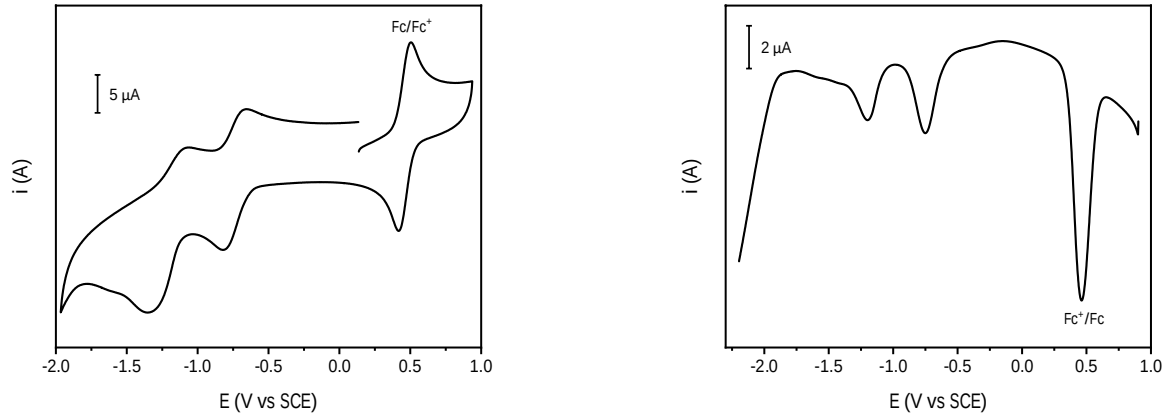

Figure S35. CV (left, scan rate: 200 mV s^{-1}) and DPV (right, scan rate: 20 mV s^{-1}) of a 2.4 × 10^{-4} M solution of $R6_{LL}$ in CH_2Cl_2.

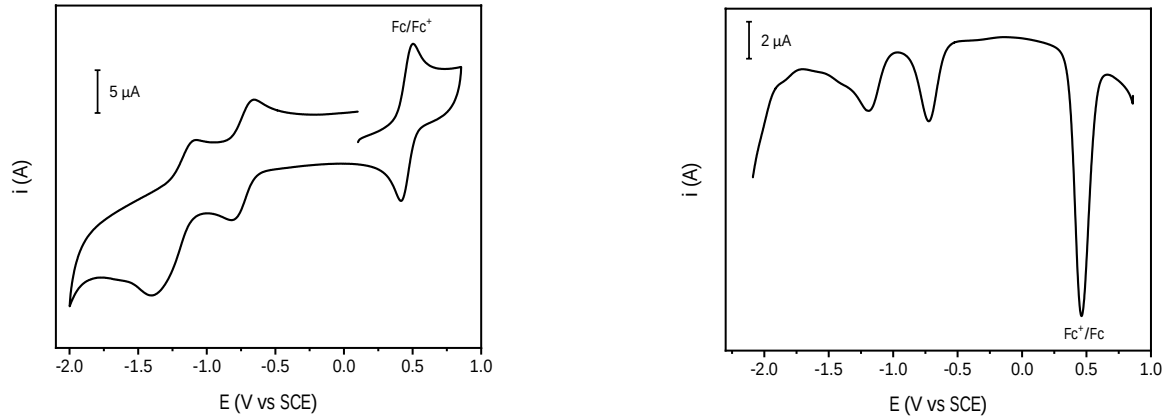

Figure S36. CV (left, scan rate: 200 mV s^{-1}) and DPV (right, scan rate: 20 mV s^{-1}) of a 2.3 × 10^{-4} M solution of $R6_{UL}$ in CH_2Cl_2.

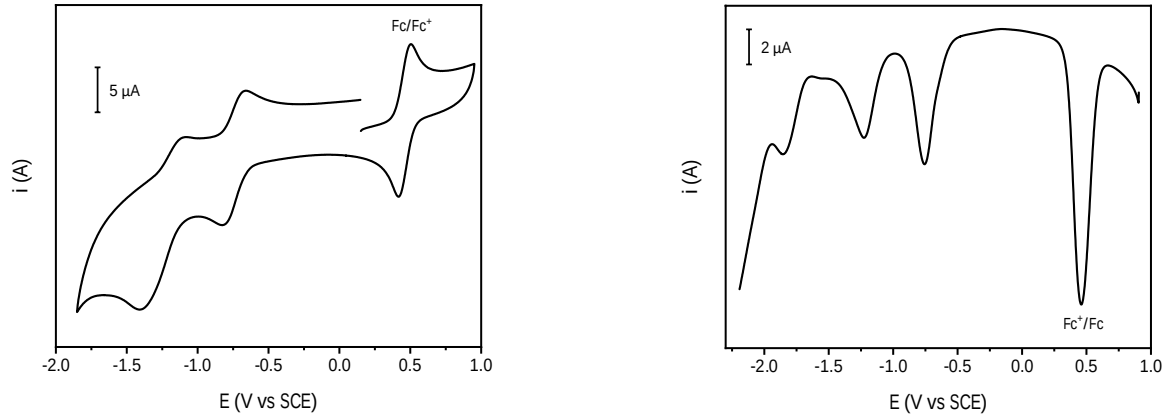

Figure S37. CV (left, scan rate: 200 mV s^{-1}) and DPV (right, scan rate: 20 mV s^{-1}) of a 2.5 × 10^{-4} M solution of $R12_{UU}$ in CH_2Cl_2. The process observed around -1.8 V is not reproducible: as it cannot be reliably assigned, it is possibly related to the presence of an impurity.

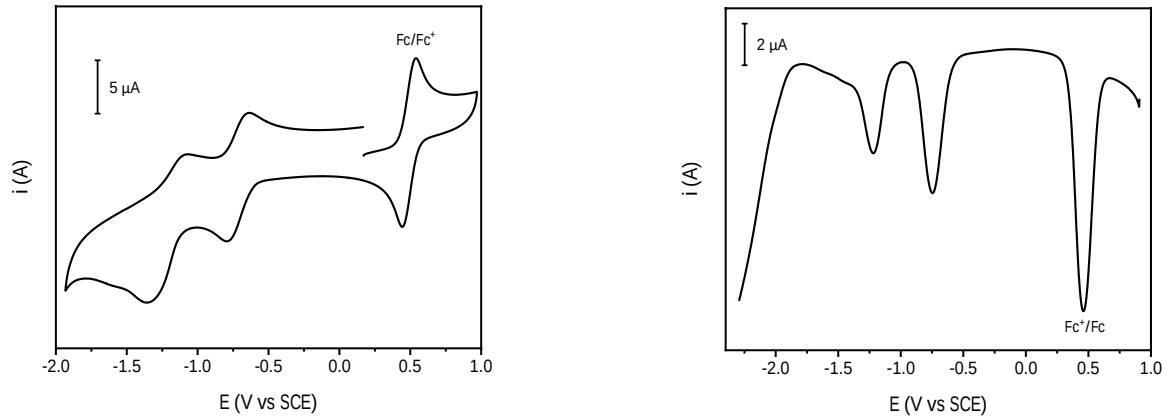

Figure S38. CV (left, scan rate: 200 mV s^{-1}) and DPV (right, scan rate: 20 mV s^{-1}) of a 2.4 × 10^{-4} M solution of $R6_{LL}$ in CH_2Cl_2.

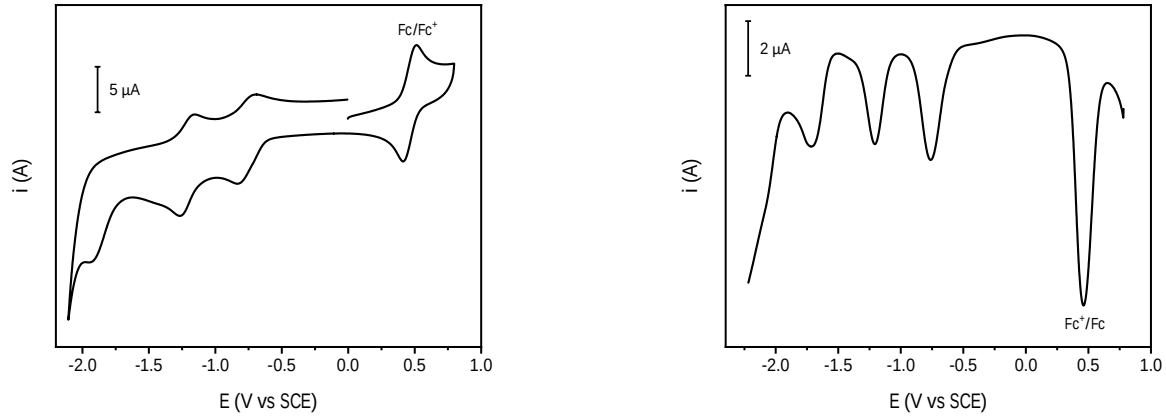

Figure S39. CV (left, scan rate: 200 mV s^{-1}) and DPV (right, scan rate: 20 mV s^{-1}) of a 2.3 × 10^{-4} M solution of $R6_{UL}$ in CH_2Cl_2. The process observed around -1.7 V is not reproducible: as it cannot be reliably assigned, it is possibly related to the presence of an impurity.

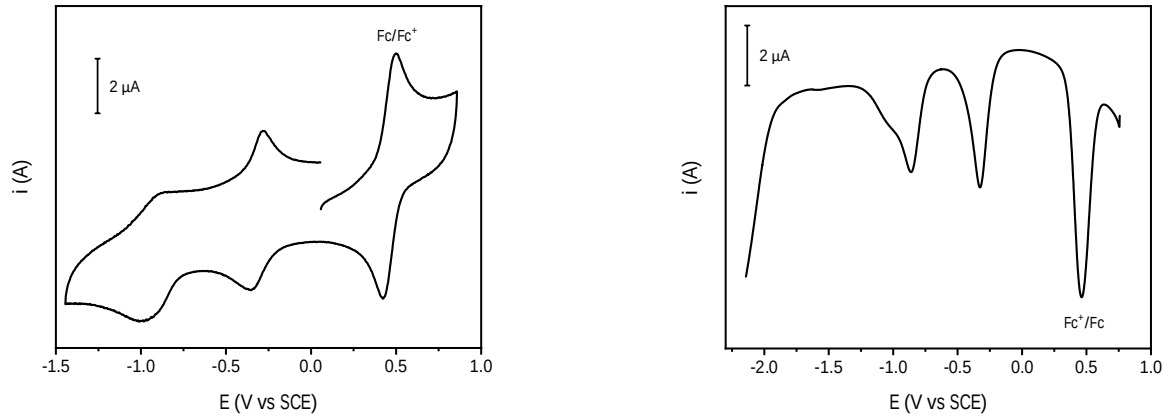

Figure S40. CV (left, scan rate: 200 mV s^{-1}) and DPV (right, scan rate: 20 mV s^{-1}) of a 9.6 × 10^{-5} M solution of dumbbell 7a in CH_2Cl_2.

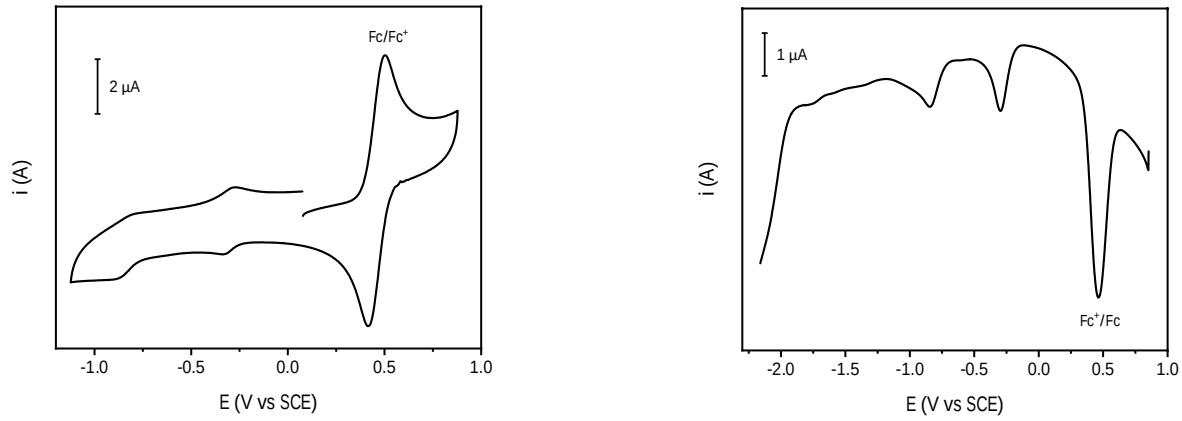

Figure S41. CV (left, scan rate: 200 mV s^{-1}) and DPV (right, scan rate: 20 mV s^{-1}) of a 5.7 × 10^{-5} M solution of dumbbell 7b in CH_2Cl_2.

References

1. J. J. González, R. Ferdani, E. Albertini, J. M. Blasco, A. Arduini, A. Pochini, P. Prados and J. De Mendoza, Dimeric capsules by the self-assembly of triureidocalix[6]arenes through hydrogen bonds, *Chem. - Eur. J.*, 2000, 6, 73–80.
2. V. Zanichelli, G. Ragazzon, A. Arduini, A. Credi, P. Franchi, G. Orlandini, M. Venturi, M. Lucarini, A. Secchi and S. Silvi, Synthesis and Characterisation of Constitutionally Isomeric Oriented Calix[6]arene-Based Rotaxanes, *Eur. J. Org. Chem.*, 2016, 2016, 1033–1042.
3. F. Vita, M. Vorti, G. Orlandini, V. Zanichelli, C. Massera, F. Ugozzoli, A. Arduini and A. Secchi, Synthesis and recognition properties of calix[4]arene semitubes as ditopic hosts for N-alkylpyridinium ion pairs, *CrystEngComm*, 2016, 18, 5017–5027.
4. A. Arduini, R. Bussolati, A. Credi, A. Pochini, A. Secchi, S. Silvi and Margherita Venturi, Rotaxanes with a calix[6]arene wheel and axles of different length. Synthesis, characterisation, and photophysical and electrochemical properties, *Tetrahedron*, 2008, 64, 8279–8286.
5. V. Zanichelli, G. Ragazzon, G. Orlandini, M. Venturi, A. Credi, S. Silvi, A. Arduini and A. Secchi, Efficient active-template synthesis of calix[6]arene-based oriented pseudorotaxanes and rotaxanes, *Org. Biomol. Chem.*, 2017, 15, 6753–6763.